運輸省港湾技術研究所

港湾技術研究所報告

REPORT OF
THE PORT AND HARBOUR RESEARCH INSTITUTE

MINISTRY OF TRANSPORT

VOL. 23 NO. 3 SEPT. 1984

NAGASE, YOKOSUKA, JAPAN

港湾技術研究所報告 (REPORT OF P.H.R.I)

第23巻 第3号 (Vol.23,No. 3) 1984年9月 (Sept.1984)

目　　次 (CONTENTS)

REPORT OF THE PORT AND
HARBOUR RESEARCH INSTITUTE
Vol. 23, No. 3 (Sept. 1984)

1. Multiple Longshore Bars Formed by Long Period Standing Waves

Kazumasa KATOH*

Synopsis

Crescentic bars and multiple longshore bars are often formed on the sea bottom in the nearshore zone. Search for the origin of these topographies has recently become very important for the understanding of the mechanism of nearshore currents, deformation of nearshore topographies and several related phenomena in the surf zone.

Long waves of about 1 to 3 minutes in period have attracted the attention of several researchers as a possible origin of multiple longshore bars. They have proposed theories such that the long period waves of standing mode are formed in the nearshore zone; bed materials are transported from the nodes to the antinodes of these standing waves by their drift velocity; and thus the longshore bars are built at the antinodes of long period standing waves. These are, however, still hypothetical because they have the following shortcomings.

a) The orbital and the drift velocities of usual long period waves are not large enough to be capable of moving the bed materials.
b) Energy of long period waves in the field must be concentrated in a narrow frequency band.

In this paper, a new theory is derived and the field data of two dimensional multiple longshore bars are analyzed, in order to give satisfactory explanations for the above two items.

First, the analysis of the actual wave data shows that the long period waves do not exist independently but coexist with the incident wind waves. Then, both the incident waves and the long period wave on a beach are taken into account as the external forces for sand transport in the theoretical analysis. As a result, the formation of the multiple longshore bars are explained such that the bed materials suspended by the incident waves are transported to the locations of antinodes of the standing waves by the drift velocity of the latter waves. The analysis of the actual data of Hakui Beach in Japan shows that there exist the long period waves of 0.01Hz in frequency, whose antinodes are corresponding to the locations of the multiple longshore bars. Furthermore, the long period wave height, their predominant frequency, and the mean bottom slope between the shoreline and the most offshore-side trough satisfy the critical equation for breaking of the long waves which was presented by *Shuto*. The multiple longshore bars at Hakui Beach have been formed and amplified by the existence of perfectly reflected long period waves with the prevailing frequency.

* Chief of Storm Surge and Tsunami Laboratory, Hydraulic Engineering Division

港湾技術研究所報告
第23巻　第3号　(1984. 9)

1.　反射定常波による多段沿岸砂州の形成

加　藤　一　正*

要　　旨

沿岸部に三日月砂州や多段の沿岸砂州がしばしば存在することは，よく知られている。これらの成因を探っていくことが，砕波帯内の諸現象，海浜流，沿岸地形変化を理解するために重要となっている。

これらの有力な成因として，周期が1～数分の長周期波の存在が注目され，種々の理論検討の結果，長周期波の質量輸送により底質が長周期波の腹の位置に運ばれ，沿岸の規則的な地形が形成されると説明されている。しかしながら，従来の考え方では，

a）長周期波には底質を移動させるだけの流速がない。

b）現地に存在する長周期波が狭い周波数帯内にエネルギー集中していなければならない。

等に対して十分な説明ができておらず，いまだ仮説的であるとされている。

そこで，本論文では，上記2項目を明確にするために，二次元的な地形である多段の沿岸砂州について理論的検討，現地データの解析を行った。

まず，最初に現地波浪データを基にして，長周期波は単独で存在するものではなく，入射波とともに共存することを示した。そこで，入射波と長周期の反射定常波を考慮に入れて理論解析を行った結果，多段沿岸砂州は，入射波によって浮遊した砂が反射定常波の質量輸送によってその腹の位置に運ばれて形成されると説明された。次に現地の波浪と多段沿岸砂州地形を解析したところ，多段沿岸砂州の位置に腹が対応する反射定常波の周波数と波高，海底勾配は，長波の砕波限界式を満足するものであることが分かった。そして，海底勾配と長周期波の波高によって規定される砕波限界周波数の反射定常波が，多段沿岸砂州の形成において重要な役割を果していることが分かった。

* 水工部　高潮津波研究室長

Contents

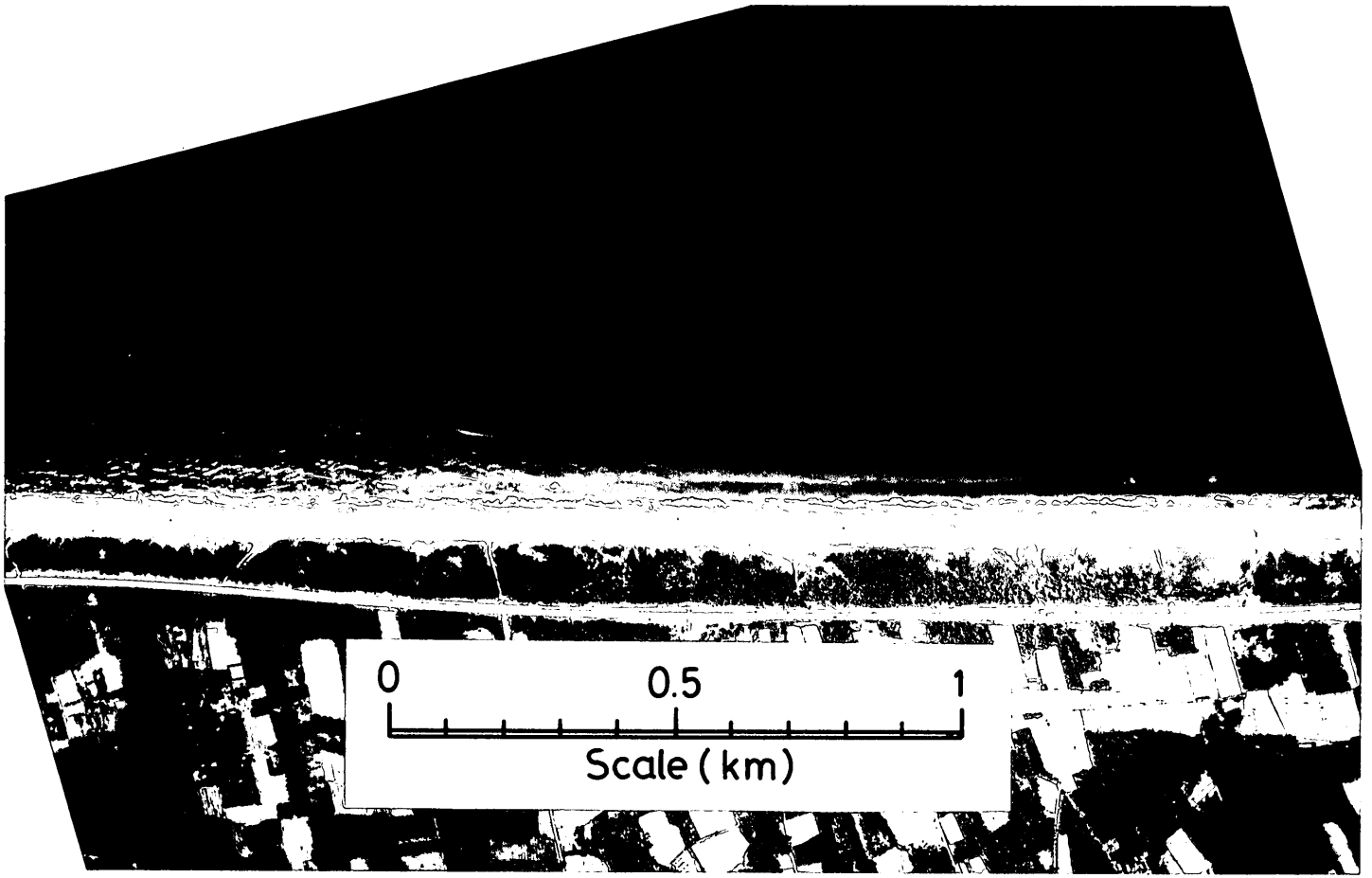

(a) Sept. 6, 1975 (11h. 29m.). Reference point No.42 to No.54.

Photograph 1 Multiple longshore bars at Hakui Beach, Japan taken by the Geographical Survey Institute, Ministry of Construction. Number of reference points below each photograph correspond to those in Fig.14.

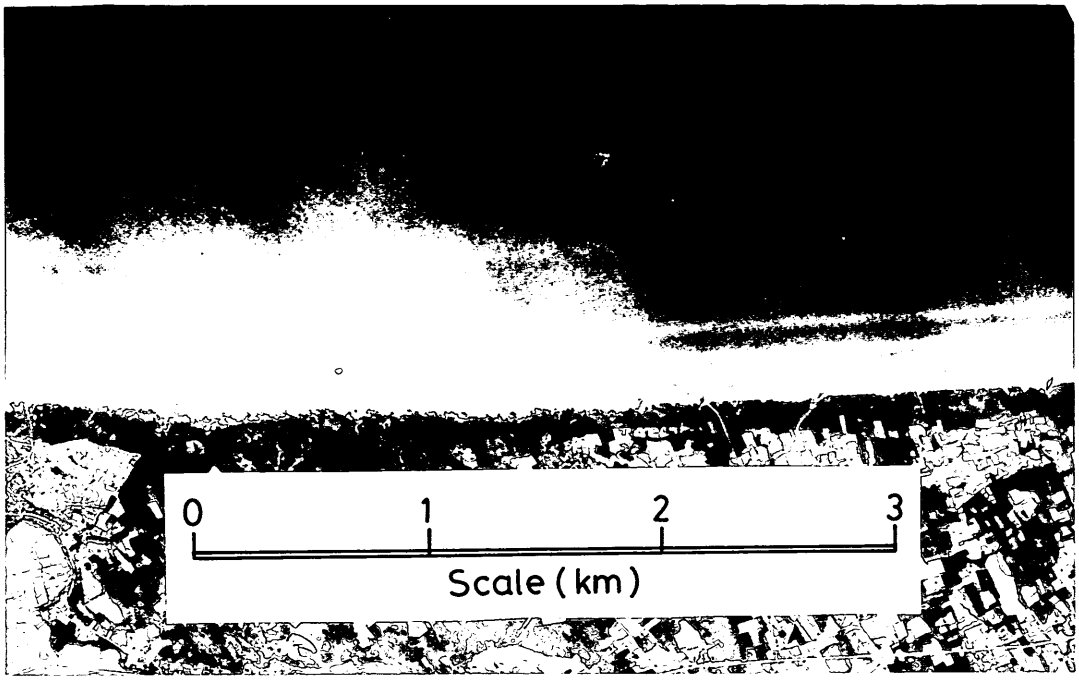

(b) Sept. 30, 1963 (10h.59m.). Reference point No.27 to No.50.

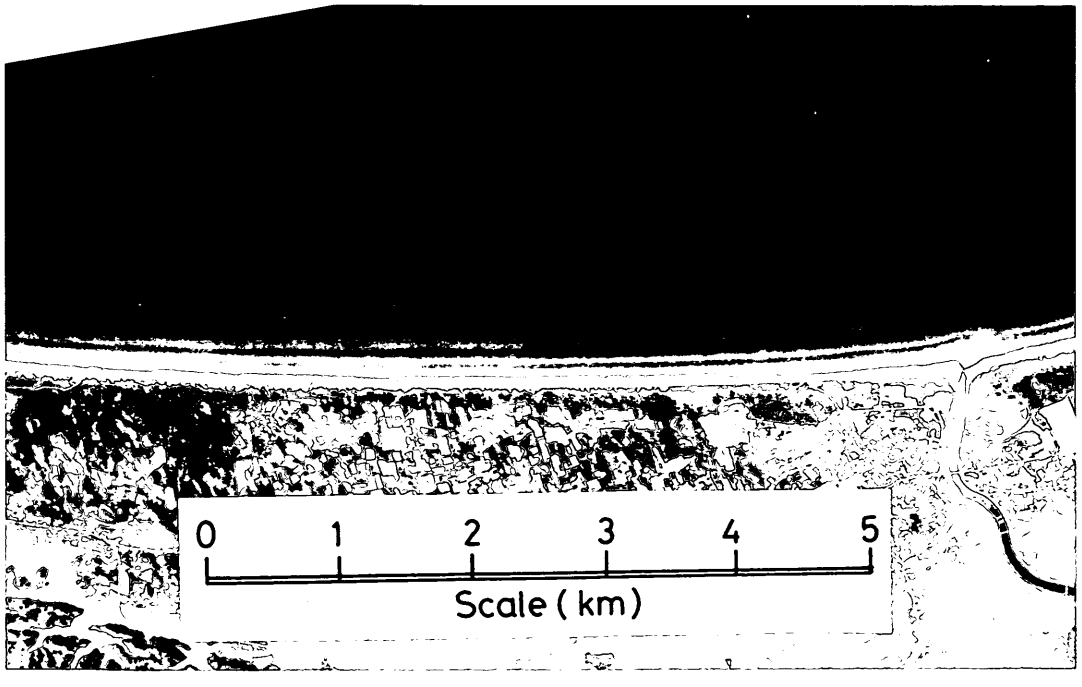

(c) Sept. 28, 1967 (10h.18m.). Reference point No.29 to No.68.

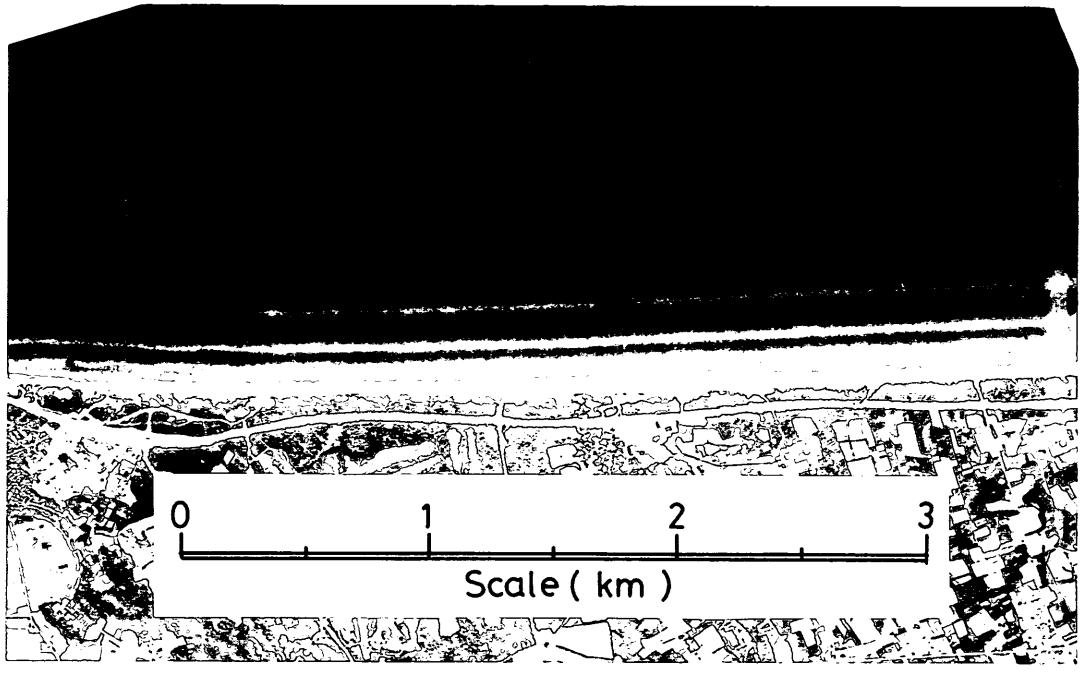

(d) June 6, 1972 (9h 36m.). Reference point No.27 to No.49.

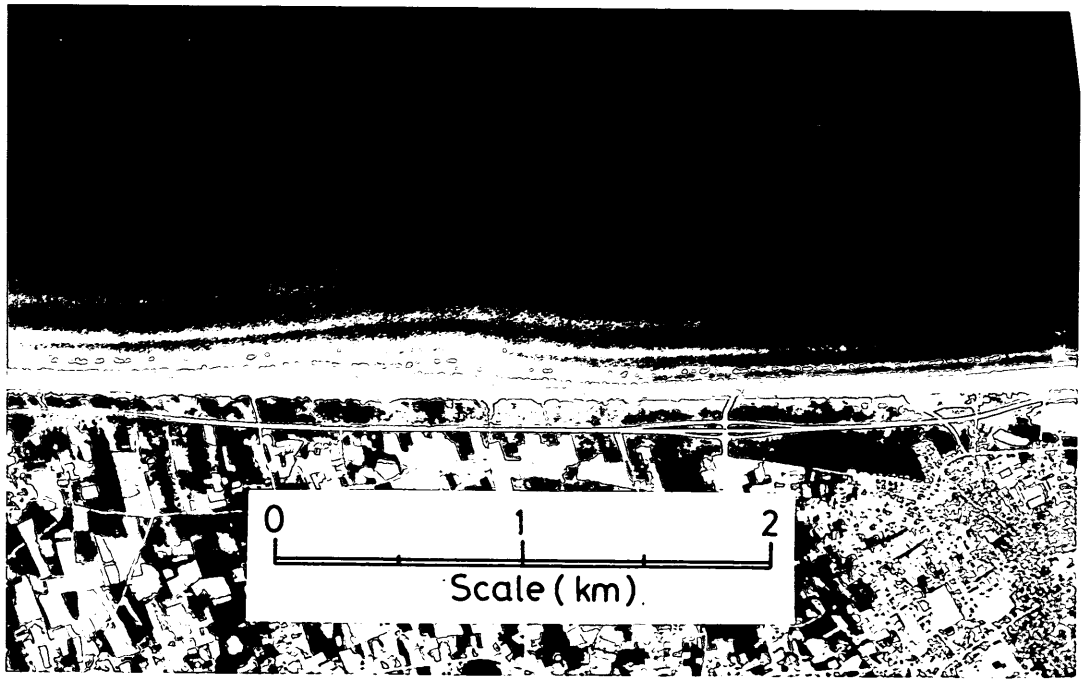

(e) May 12, 1982 (9h. 46m.). Reference point No.41 to No.63.

1. Introduction

Waves coming from the offshore break in a zone of shallow water at their final stage. Within the surf zone, the energy of wave motion are transferred into those of currents and intense turbulence. The inter-relationship between the fluid motions and the sediment movement or other phenomena of diffusion in the surf zone is quite a complex problem. Surprisingly, however, the nature often creates the rhythmic topographies such as multiple longshore bars, crescentic bars, ripples, cusps and so on, under these complicated and irregular fluid motions. Search for the origin of these topographies has recently become very important for the understanding of the mechanism of nearshore currents, deformation of nearshore topographies and several related phenomena in the surf zone.

Jetties and detached breakwaters are constructed in the nearshore zone for the purpose of preventing of beach erosion. These structures are mostly arranged in regular intervals of one to several hundred meters in space. The scales of arrangements of these structures agree well with those of nearshore rhythmic undulating topographies such as the crescentic bars, the multiple longshore bars, and the cusps no the shoreline. *Hom-ma* and *Sonu*(1962) stressed that the interaction between nearshore undulations and the structures should be studied in order to provide a good design criterion of these structures. It has passed more than twenty years since they pointed out it, but such criterion has never been established yet, because we do not have satisfactory explanation for the origin of nearshore undulations.

Long waves of about 1 to 3 minutes periods have attracted the attention of several authors as a possible origin of large scale undulations. *Bowen* and *Inman* (1971) showed theoretically that standing edge waves can be the origin of the formation of crescentic bars in regions of small tidal range, the bars having a longshore wavelength of one-half that of the edge waves. In their analysis, the velocity field associated with the edge waves on a sloping beach were examined. They concluded that the net drift velocities due to the standing edge waves, just above the bottom boundary layer, transport bed materials to the zone of nearly zero drift velocity and deposit the bed materials there. Of course, it was theoretically shown that the zone of nearly zero drift velocity forms the area of crescentic formation in space.

Short (1975) analyzed the actual data of multiple longshore bars at the beaches of North Alaska. He showed that the measured spacing of bar crests agreed with the spacing of antinodal or nodal points of the standing waves which were measured by *Suhayda*(1975).

Bowen(1980) showed that, starting from the *Bagnold Model*(1962, 1963) for sediment transport, a model for wave-induced on-offshore transport on a beach can be derived. By using this model, he explained that the multiple longshore bars are more likely to be noticeable on steep beaches where the reflection coefficient tends to be larger.

Holman and *Bowen* (1982) theoretically examined the interaction of two edge waves in detail. The drift velocities were calculated and the above model by Bowen was used to predict the three dimensional beach topography such as welded sand bars that would be in equilibrium with these flow patterns. They suggested that other three dimensional, complex, rhythmic topographies could also be explained by the same analyses with three or more wave systems.

Carter, *Liu* and *Mei* (1973) theoretically studied on the drift velocities due to

the partial standing wave. It was shown that the directions of drift velocities depend on the reflection coefficient, which are the same directions at the all points as that of the incident wave when the reflection coefficient is less than 0.414. Therefore, bed materials will not be transported to the points of antinode of the partial standing waves in the case of the reflection coefficient less than 0.414.

However, as pointed out by *Sonu* (1972), *Mizuguchi* (1979) and *Holman* (1981), the past theories cannot overcome the following problems in explaining the mechanism of multiple bars formation.

(a) The orbital and drift velocities of usual long period waves is not large enough to be capable of moving the bed materials.

(b) The energy of long period waves in the field must be concentrated in a narrow frequency band.

In this paper, in order to give satisfactory explanations for the above two problems, the features of long period waves at Hakui Beach in Japan, where multiple longshore bars exist, are examined at first. After that, a theory is derived by following the approach by *Bowen* (1989) by taking into account both incident and long period wave characteristics, and then the actual data of two dimensional multiple longshore bars at Hakui Beach are analyzed.

2. Long Period Waves at Hakui Beach Facing the Japan Sea

2.1 Detection of Multiple Longshore Bars by Utilization of Aerial Photographs

An aerial photograph, if taken under favorable conditions, can show an interesting picture of submerged topographies in a distinct contrast made by the bright tone of a shallow bar crest or a shoal, against the dark background of a deep trough or a rock bottom. Because of this characteristic, many researchers utilized aerial photographs in order to investigate the sizes, configurations and other features of submerged topographies (e. g., *Hom-ma* and *Sonu* 1962, *Sonu* 1968, *Bowen* and *Inman* 1971, *Lau* and *Travis* 1973, *Wright*, *Thom* and *Chappell* 1978, *Davis* 1978, *Barusseau* and *Saint-Guily* 1981, *Holman* and *Bowen* 1982, *Short* and *Hesp* 1982), and many of them reproduced the typical examples of the aerial photographs of submerged topographys on their papers.

In the present study, first of all, aerial photographs along the coast lines of Japan have been examined to detect and select a beach where the formation of longshore bars is most prominently found. For this purpose, about six thousands of aerial photographs, which have already been used for analyzing the shoreline changes (*Tanaka et al.* 1973, 1974a, 1974b, 1977, *Ozasa* 1977) and have been filed in the Port and Harbour Research Institute, were inspected. These photographs were taken by the U.S. Air Force between 1946 and 1948 and by the Geographical Survey Institute, Ministry of Construction, after 1961.

Figure 1 shows the locations in Japan where submerged bars can be recognized in the aerial photographs. The configurations of bars detected are ample in variation such as the bars parallel to the shoreline, the rhythmic crescentic bars in the longshore direction, and the entirely complicated ones. Among them, the multiple longshore bars formed at Hakui Beach, Ishikawa prefecture, were the most beautiful and the simplest ones of two dimensional character. In order to simplify the analytical treatments, Hakui Beach has been chosen for examination in this paper. Typical examples of the multiple longshore bars in the aerial photographs are shown in Photographs 1(a)-(e), which will be analyzed in Section **4.1**.

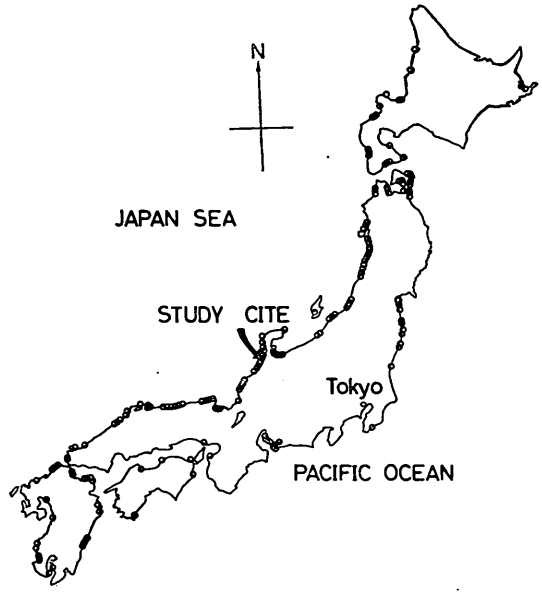

Fig. 1 Locations where submerged bars can be recognized in aerial photographs, denoted with small circles.

2.2 Tides and Waves

Hakui Beach is located in the north end of an essentially straight coast of about 60 kilometers long facing the Japan Sea. This beach is famous in Japan for the sightseeing with enjoying a drive on a foreshore, where a slope is gentle and this sandy beach is rigid enough for driving (see Photograph 2). The waves are being measured during twenty minutes of every two hours at the depth of 20 meters below the datum line near Kanazawa Port which is located about 30 kilometers southwest from Hakui Beach (see Fig.2). The tidal level is also being observed in Kanazawa Port.

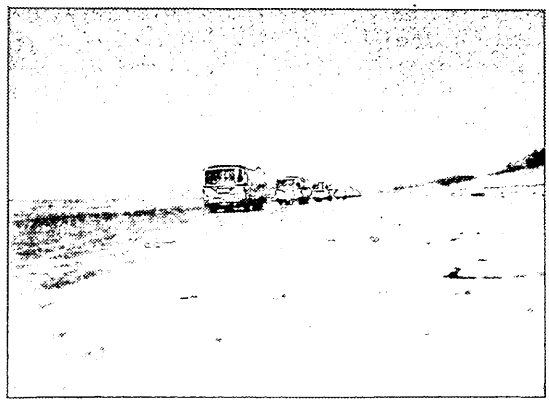

Photograph 2 Hakui Beach (with the courtesy of prefectual government of Ishikawa).

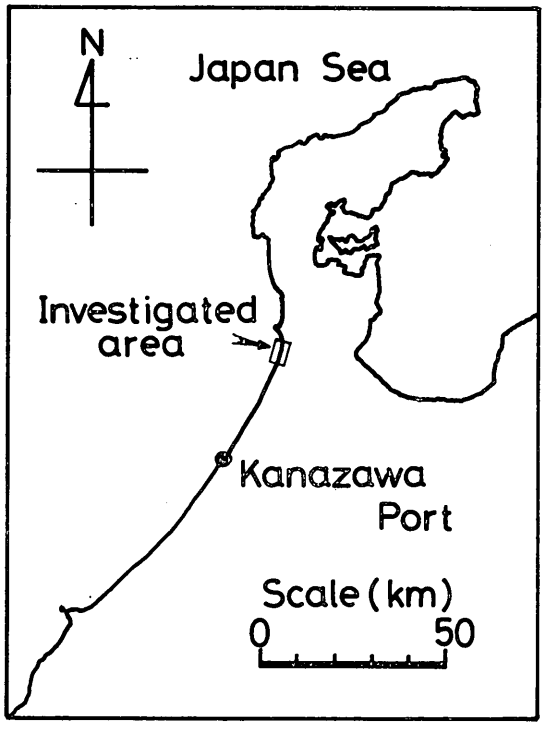

Fig. 2 Investigated beach, Hakui Beach, Japan.

The mean value and the standard deviations of tidal level for every month have been calculated with the tidal level data of every hour during one year from October 1982 to September 1983 and shown in Fig. 3. The monthly mean tidal level varies with a amplitude of about 20 centimeters and with a period of one year. It is rather high during a period from July to October, while it is rather low from February to April. The standard deviation of tidal level is about 10 centimeters through the

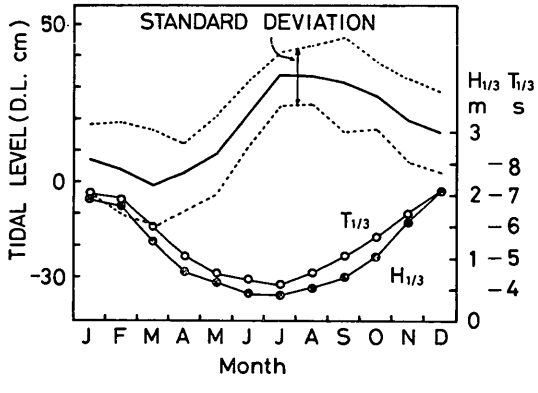

Fig. 3 Annual variations of significant wave height and period, tidal level and standard deviation of tidal levels.

year, which means that the tidal range is very small. The tidal constituents are K_1=5cm, O_1=5cm, M_2=6cm and S_2=2cm. The monthly mean significant wave height and period during ten years from 1970 to 1979 (*Takahashi*, *Hirose*, *Sugahara* and *Hashimoto* 1981) are also shown in Fig. 3. The monthly mean significant wave height is high (about 2 meters) during the winter period from December to February, while it is low (about 0.5 meter) during the summer period. According to these data, it is assumed in the data analyses in Chapters **3** and **4** that the mean tidal level during the period of high waves is 0.16 meter above the datum line and the tidal range can be neglected.

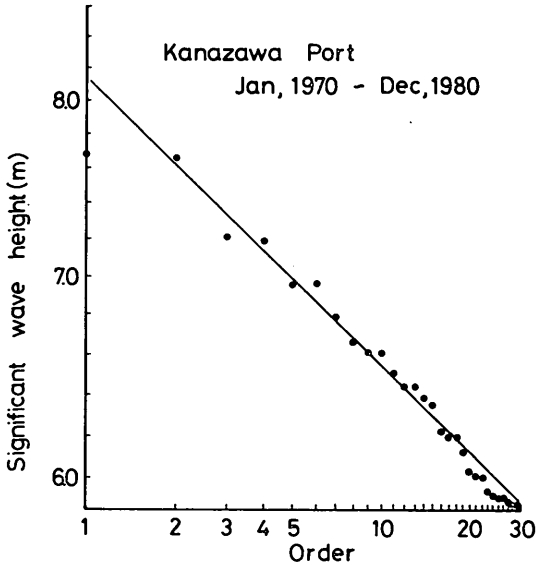

Fig. 4 Largest thirty values of the significant wave height at Kanazawa Port during ten years from 1970 to 1979.

Figure 4 shows the largest thirty significant wave heights during ten years from 1970 to 1979 (*Takahashi et al.* 1981). It can be noticed that the significant wave height greater than 6 meters ocurred nearly twice a year on the average at Hakui Beach.

Bed materials were sampled in May 1983 along three measurement lines normal to the shoreline. On each measurement line, the sampling points were selected at five points from the backshore to the depth of 5 meters, including the locations of a trough and a summit of bar. A result of the analysis on the grain size distribution shows that the medium diameter of sand is 0.17 millimeter and remains constant irrespective of locations.

2.3 Long Period Waves

Spectral analyses have been done for the case of the significant wave height exceeding 2 meters among the data obtained in the year of 1982. A number of records used for these analyses is 505, which is equivalent to the accumulated duration of about 42 days because wave records were taken twelve times a day. A sampling

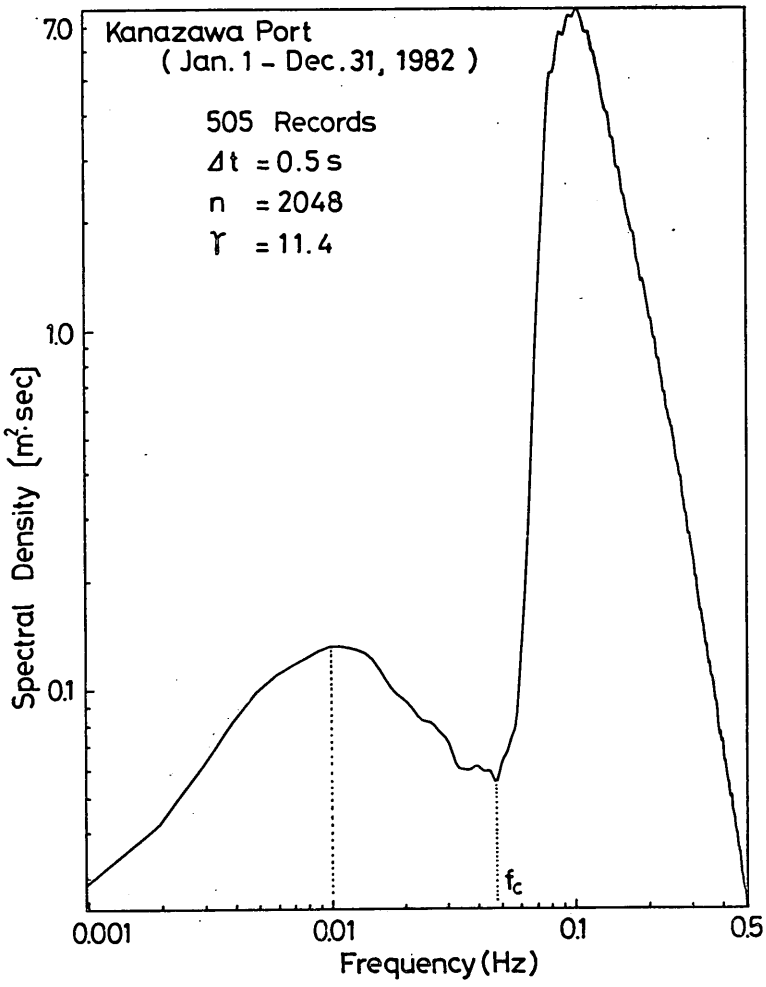

Fig. 5 Averaged spectral density of 505 records of wave data, equivalent to the period of about 42 days, which were exceeding 2 meters in the significant wave height.

interval of data is $\Delta t=0.5$ second and a number of data is $N=2048$ for each record. The equivalent degree of freedom with a filter used for smoothing is $r=11.4$.

Figure 5 shows the arithmetic average of spectral densities of the whole 505 records. According to Fig. 5, there are two spectral peaks. One is very sharp at the frequency of about 0.1 Hz, which corresponds to that of incident wind waves. Another is flatter and lower than the former in shape and in density respectively, but still recognizable at the frequency of about 0.01 Hz. That is to say, the long period waves of about 100 seconds in period coexist with the incident wind waves at Hakui Beach.

Figure 6 shows the changes of the significant wave height, period and spectral density of waves in a storm condition during the period from January 28th to 30th,

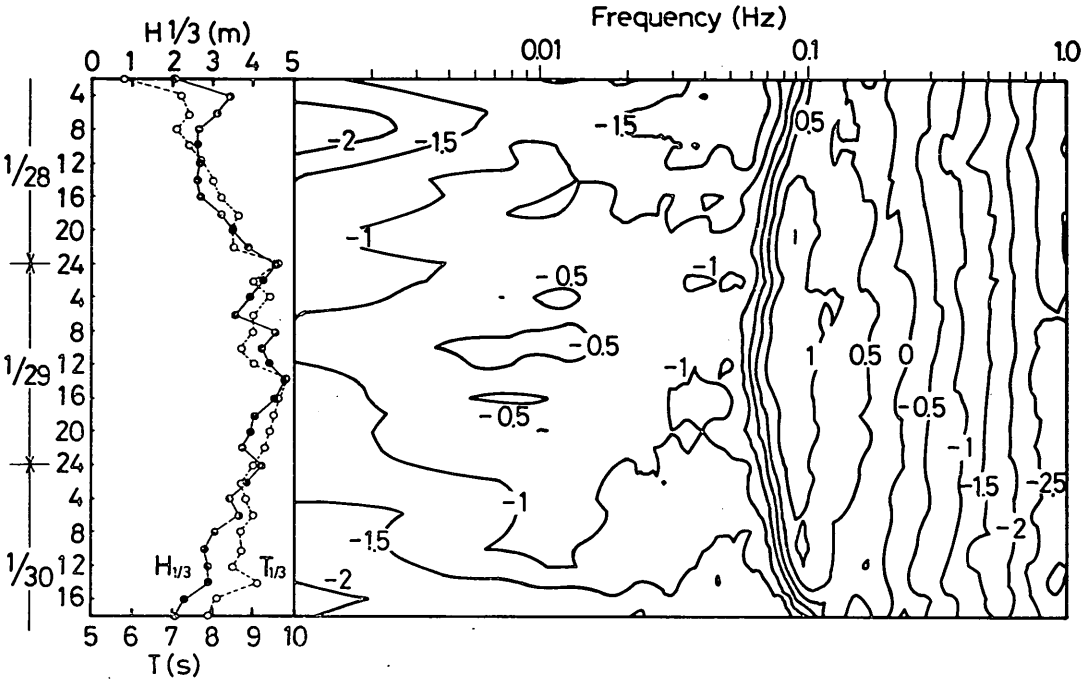

Fig. 6 Changes of significant wave height, period and spectral density of waves in the storm condition during the periods of January 28 to 30, 1982 at Kanazawa port. A figure on each contour line represents the decimal exponent of spectral density in the units of m^2s.

1982 ; the spectral density is presented in the form of contour map. As seen form this example, the energy density of the long period waves at the frequency of around 0.01 Hz increases and decreases in proportion to that of the incident waves at the frequency of 0.1 Hz.

Similar results have already been pointed out by a few researchers. For examples, *Munk* (1949, 1962), who was the first to quantitatively detect the existence of the long period waves in the field, reported that the ratio of the significant wave height of long period waves to that of incident waves was about 1/10 to 1/11. *Tucker* (1950), who also observed the long period waves at almost the same time, reported that the ratio was about 1/16. Figure 7 shows the relation between the wave heights of long period waves (H_L) and those of incident waves (H_S), which were calculated respectively by the following equations based on the result of each spectra analysis for 505 records.

$$H_L = a\left(\int_0^{f_c} S(f)\,df\right)^{1/2}, \qquad (1)$$

$$H_S = a\left(\int_{f_c}^{\infty} S(f)\,df\right)^{1/2}, \qquad (2)$$

where f is the frequency, $S(f)$ is the spectral energy density and f_c is the threshold frequency of 0.047 Hz as shown in Fig. 5, at which the value of $S(f)$ becomes to be the minimum. The coefficient, a, in Eqs. (1) and (2) takes a constant value of 4.004 if the wave heights are distributed according to the Rayleigh

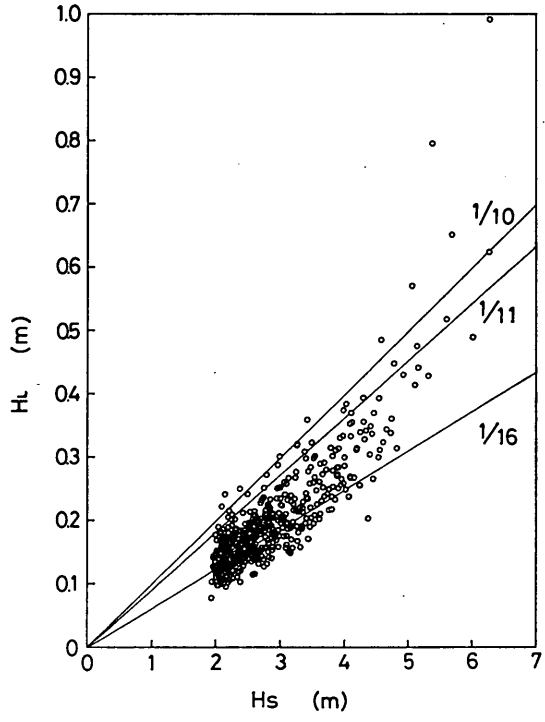

Fig. 7 Relation between the wave height of long period waves and those of incident waves at Kanazawa Port in 1982.

distribution, but the value of 3.8 is employed for a in this paper because the latter is considered more appropriate for the actual wave data as pointed out by *Goda* (1979). Solid lines in Fig. 7 indicate the ratio of the wave heights of long period waves to that of incident waves being 1/10 and 1/11 by *Munk*, and 1/16 by *Tucker*. Most of the data are plotted in the range between the relations given by *Munk* and *Tucker*, but there is a tendency that the data scatter around the line of 1/16 when the height of incident waves are small and they shift to the lines of 1/11 and 1/10 with the increase of the incident wave height.

Goda (1975) considered that the difference among the ratios of *Munk* and *Tucker* was due to the difference of the water depth where the waves were measured. Then, based on the wave data measured both in the surf zone and offshore of Ooarai Beach, Niigata Beach and Miyazaki Beach in Japan, he took the water depth into account and empirically obtained the following relation :

$$\frac{\zeta_{rms}}{(\eta_{rms})_0} = \frac{0.04}{\sqrt{\frac{H_s}{L_0}\left(1+\frac{h}{H_s}\right)}}, \qquad (3)$$

where ζ_{rms} and $(\eta_{rms})_0$ are the root-mean-square value of the wave profiles of long period waves and incident waves, respectively, h is the water depth and L_0 is the significant wave length in deep water. Values of *Goda's* parameters have been calculated for 505 records of wave data exceeding 2 meters in the significant wave height and they are plotted in Fig. 8. In the calculation, the water depth was

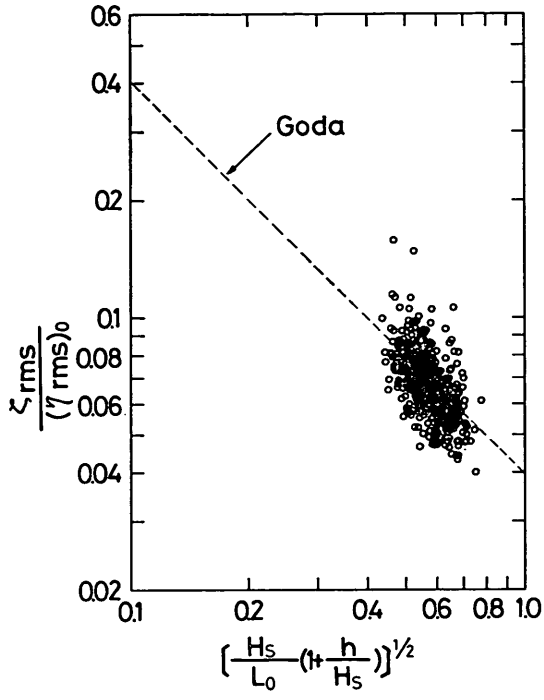

Fig. 8 Values of *Goda's* parameters for waves at Kanazawa Port in 1982.

assumed to be $h=20.16$ meters and use was made of Eq. (2) and the following relations :

$$\frac{\zeta_{rms}}{(\eta_{rms})_0}=\left(\frac{\int_0^{f_c}S(f)df}{\int_{f_c}^{\infty}S(f)df}\right)^{1/2}, \tag{4}$$

$$L_0=\frac{g}{2\pi}\cdot T_s^2, \tag{5}$$

$$T_s=1.11\cdot\left(\frac{\int_{f_c}^{\infty}S(f)\,df}{\int_{f_c}^{\infty}f^2\cdot S(f)df}\right)^{1/2}, \tag{6}$$

As seen in Fig. 8, the data scatter around a broken line which indicates *Goda's* relation (Eq. 3). That is to say, the wave height of long period waves at Hakui Beach are not particularly different but are almost the same as those at the other beaches in Japan.

Figure 9 shows the occurrence frequencies of the wave height of long period waves which were estimated with the data of 505 records by using Eq.(1). According to this figure, the wave height of long period waves is generally less than 30 centimeters and the mode of the long period wave height is about 16 centimeters with the peak frequency of 25 percent.

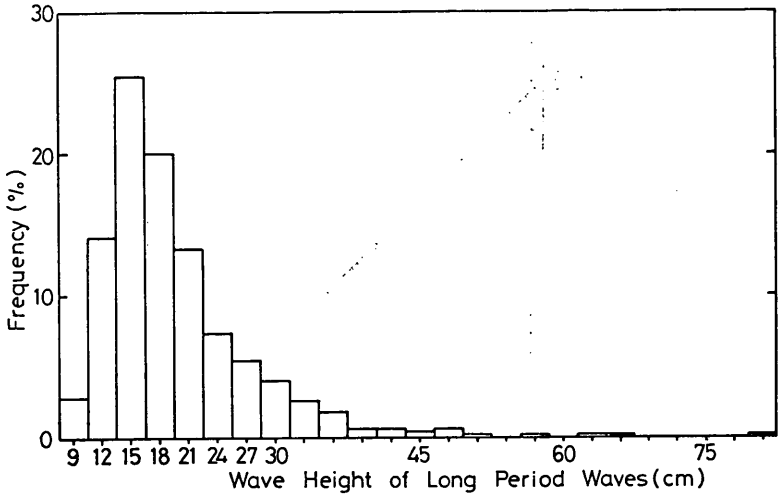

Fig. 9 Occurrence frequencies of wave heights of long period waves at Kanazawa Port in 1982

3. Theoretical Investigation on Relation between Long Period Waves and Multiple Longshore Bars

3.1 Form of Sand Movements in Storm Wave Conditions in the Field

By substituting the water velocities due to orbital wave motions into *Bagnold's* equations(1962) for the suspended load transport and the bed load transport, *Bowen* (1980) theoretically obtained the equations of net transport rates of the suspended load and the bed load. By utilizing these equations, he examined the ratio of the net transport of the suspended load to that of the bed load. According to his result, this ratio depends on a paramenter of U_0/ω, where U_0 is the horizontal component of maximum velocity on the bottom and ω is the settling velocity of bed materials, and the suspended load would be significant when the value of U_0/ω is greater than about 15.

Shi-Leng (1981) and *Irie*, *Nadaoka*, *Kondo* and *Terasaki* (1984) carried out the two-dimensional experiments on the deformations of bottom topography due to standing waves. They found out the interesting phenomena that there are two different patterns in the bed material accumulation. One is that the bed materials move from nodes to antinodes of standing waves and the seabed is scoured near the nodes and accretes at the antinodes. The other is the reverse pattern. Moreover, they revealed that these opposite patterns can be well explained by the parameter of U_0/ω and that the former pattern occurs when the value of U_0/ω is greater than 10. *Irie et al.* investigated in detail the structures of fluid motion, such as the orbital velocity, the mean velocity, the strength of turburence and Eulerian drift velocity, due to the standing waves by means of a laser doppler current meter. After that, *Irie et al.* gave an explanation for these experimental results that the suspended load is significant if $U_0/\omega>10$ and it is transported by the drift velocity due to the standing waves which directed from the nodes to the antinodes.

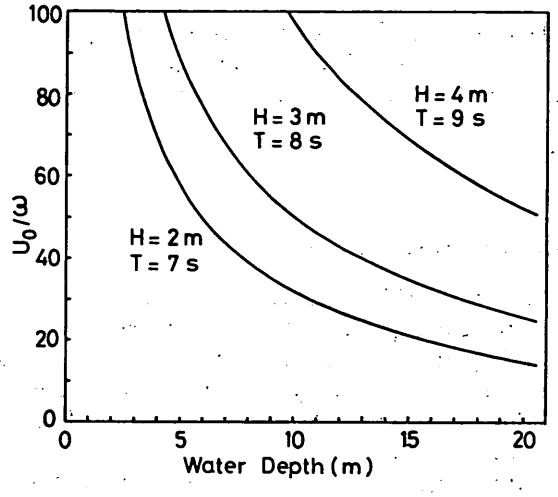

Fig. 10 Ratio of the maximum orbital velocity on the bottom to the settling velocity of bed material in storm wave conditions.

Since U_0/ω is considered to be the important parameter governing the form of sand movements, as mentioned above, the value of U_0/ω at Hakui Beach has been estimated in the storm conditions with the significant wave height greater than 2 meters. Figure 10 shows the relation between U_0/ω and the water depth shallower than 20 meters for three wave conditions. Wave heights in this figure correspond to those at the wave observation point (the water depth is 20.16 meters). In the calculation, the change of the wave height due to wave shoaling is estimated by the small amplitude wave theory and the settling velocity is obtained by using *Rubey's* equation under the conditions that the diameter and the specific gravity of bed materials are 0.17 millimeter and 2.65, respectively, the water temperature is 15 degrees in the centigrade scale and the specific gravity of sea water is 1.03. From Fig. 10, it is obvious that in the storm conditions the value of U_0/ω is greater than 40 at the depth shallower than 7 to 8 meters, where multiple longshore bars are formed on the seabed (see Fig. 15 for typical seabed profiles).

By referring to the theoretical findings by *Bowen* (1980) and experimental evidences by *Shi-Leng* (1981) and *Irie et al.* (1984), it can be inferred that the suspended load transport must be more significant than the bed load transport in the storm conditions at Hakui Beach.

3.2 Suspended Sand Transport by both Incident and Long Period Waves

According to the foregoing considerations, important features of Hakui Beach related to the development of the theory of multiple longshore bars formation are as follows :

(a) the long period waves of about 100 seconds in period coexist with the incident wind waves,

(b) the suspended transport is predominant in the storm conditions.

For the sake of simplicity, we shall here treat a two-dimensional situation, where waves are normally incident to the shoreline and the bed materials are transported

only on-offshore.

From the former feature (a), the water particle velocity due to incident waves and the velocity due to long period waves are combined to estimate the total velocity, u, which is defined as positive seawards, as below :

$$u=U_0+U_1, \tag{7}$$

$$U_0=u_0\cos\sigma t, \tag{8}$$

$$U_1=u_1+u_2\cos 2\sigma t+u_{B0}\sin\sigma_B t+u_{B1}, \tag{9}$$

where $u_0\cos\sigma t$ and u_1 are the orbital velocity and the drift velocity of incident waves, respectively, $u_2\cos 2\sigma t$ represents the velocity asymmetry of incident waves (the velocity is greater beneath the wave crest than beneath the wave trough), and $u_{B0}\sin\sigma_B t$ and u_{B1} are the orbital velocity and the drift velocity of long period waves, respectively. Moreover, σ and σ_B are the angular frequencies of incident waves and long period waves, respectively.

From the latter feature (b), it is decided to use the formula for suspended load transport on a sloping beach derived by *Bagnold*(1962) as

$$i_s=\frac{\varepsilon_S\cdot C_D\cdot\rho\cdot u^3\cdot|u|}{\omega-u\beta}, \tag{10}$$

where ε_S is the efficiency (the ratio of energy to be consumed for sand movement in suspension to the total energy of fluid motion), C_D is the drag coefficient, ρ is the water density, ω is the settling velocity and β is the beach slope. The rate of suspended load transport i_S is also defined positive seawards. Equation (10) has been employed by *Bowen*(1980) to derive the net transport rate of suspended load. We also make use of Eq. (10) in combination with Eq. (7) in order to obtain the net suspended load transport under the situation considered.

Generally speaking, the amplitude of the orbital velocity of the incident waves (u_0) is much greater than both the drift velocity (u_1) and the amplitude of the asymmetry velocity (u_2). It is also much greater than both the amplitude of the orbital velocity of long period waves (u_{B0}) and their drift velocity (u_{B1}), because the height of incident waves is larger than that of long period waves and the incident wave period is shorter than that of long period waves. Therefore, it is reasonable to assume that $U_0\gg U_1$. Based on this assumption and by substituting Eq. (7) into the term of $u^3\cdot|u|$ in Eq. (10), we have the following expansion :

$$\begin{aligned}u^3\cdot|u| &=(U_0+U_1)^3\cdot|U_0+U_1|\\ &=(U_0+U_1)^3\cdot\sqrt{(U_0+U_1)^2}\\ &\fallingdotseq(U_0+U_1)^3\cdot|U_0|\cdot\left(1+\frac{U_1}{U_0}\right)\\ &=U^3{}_0\cdot|U_0|+4U_1\cdot U^2{}_0\cdot|U_0|+6U_1{}^2\cdot U_0\cdot|U_0|+4U_1{}^3\cdot|U_0|+U_1{}^4\cdot\frac{|U_0|}{U_0}\end{aligned} \tag{11}$$

Equation (10) can be rewritten in the following form

$$i_S=\frac{\varepsilon_S\cdot C_D\cdot\rho}{\omega}u^3\cdot|u|\cdot[1-\gamma u]^{-1}, \tag{12}$$

where $\gamma=\beta/\omega$. Since the value of bottom slope β is less than 1/200 near and beyond

the most offshore-side bar (see Fig. 15), $\beta u/\omega<1$, or $\gamma u<1$, for the normal transport in the storm condition. The term of $(1-\gamma u)^{-1}$ in Eq. (12) can be expanded as in the following, by substituting Eq. (7) into it :

$$(1-\gamma u)^{-1}=1+\gamma(U_0+U_1)+\gamma^2(U_0+U_1)^2+\gamma^3(U_0+U_1)^3+\cdots\cdots. \tag{13}$$

By substituting Eqs.(11) and (13) into Eq.(12) and by taking the time average which is denoted by an overbar in expression, we have the rate of net transport over a number of wave periods as follows :

$$\begin{aligned}\overline{i_S}=\frac{\varepsilon_S\cdot C_D\cdot\rho}{\omega}\Big[&\overline{U_0^3\cdot|U_0|}+\overline{4U_1\cdot U_0^2\cdot|U_0|}+\overline{6U_1^2\cdot U_0\cdot|U_0|}+\overline{4U_1^3\cdot|U_0|}\\&+\gamma\big(\overline{U_0^4\cdot|U_0|}+\overline{5U_1\cdot U_0^3\cdot|U_0|}+\cdots\cdots\big)\\&+\gamma^2\big(\overline{U_0^5\cdot|U_0|}+\overline{6U_1\cdot U_0^4\cdot|U_0|}+\cdots\cdots\big)\\&+\gamma^3\big(\overline{U_0^6|U_0|}+\cdots\cdots\big)+\cdots\cdots\Big].\end{aligned} \tag{14}$$

This is the general expression obtained by *Bowen* (1980). Each term in the right side of Eq. (14) can be rewritten into the general form of $\overline{(\gamma U_0)^m\cdot(U_1/U_0)^n\cdot U_0^3\cdot|U_0|}$, where $m=0, 1, 2,\cdots\cdots$, $n=0, 1, 2,\cdots\cdots$. Since both values of γU_0 and U_1/U_0 are less than unity, the terms having those equal or larger than square of these parameters $(m+n\geqq 2)$ are negligible comparing with the zeroth or the first order terms (the first, the second and the fifth terms in the right side of Eq.14). Furthermore, the first term of $\overline{U_0^3\cdot|U_0|}$ vanishes when U_0 is oscillatory. Therefore, to the first order, we have

$$\overline{i_S}=\frac{\varepsilon_S\cdot C_D\cdot\rho}{\omega}\Big[\overline{4U_1\cdot U_0^2\cdot|U_0|}+\overline{\gamma U_0^4\cdot|U_0|}\Big]. \tag{15}$$

By substituting Eqs. (8) and (9) into Eq.(15), we have ultimately

$$\begin{aligned}\overline{i_S}&=\frac{\varepsilon_S\cdot C_D\cdot\rho}{\omega}\Big[\overline{4(u_1+u_2\cos 2\sigma t+u_{B0}\cdot\sin\sigma_B t+u_{B1})\cdot U_0^2\cdot|U_0|}+\gamma\overline{U_0^4\cdot|U_0|}\Big]\\&=\frac{16\cdot\varepsilon_S\cdot C_D\cdot\rho}{15\pi\omega}(5u_1\cdot u_0^3-3u_2\cdot u_0^3+\gamma u_0^5+5u_{B1}\cdot u_0^3).\\&\qquad\quad(-)\quad(-)\quad(+)\quad(\pm)\end{aligned} \tag{16}$$

The sign of each term in the right side of Eq. (16) is shown below the corresponding term. That is to say, the first term reprsents the onshore effect of the drift velocity dus to the incident waves. The second term is also negative (the onshore effect) which is due to the effect of the incident wave asymmetry. The bottom slope effect is represented by the third term. The fourth term represents the effect of drift velocity of the long period waves, whose direction depends on the relative position to the phase of those waves in the case of standing mode.

Bowen(1980) has examined an equilibrium profile, under which the net transport $\overline{i_S}$ vanishes everywhere, under the existence of only the incident waves, or $u_{B0}=u_{B1}=0$ in Eqs.(9) and (16). According to his conclusion, the gravitational effect of the third term in Eq.(16) balances with the influence of the first and the second terms for the equilibrium profile. An extreme example can be found in the offshore area where the drift velocity has more dominant effect than the wave asymmetry, and the first term would balance mainly with the third term, or

$$\gamma=\beta/\omega=-5U_1/U_0, \tag{17}$$

which yields by being integrated

$$h^3\approx(7.5\cdot\omega\cdot x)^2/g, \tag{18}$$

where h is the water depth and x is the offshore distance from the shoreline. On the other hand, in the shallow water area where the effect of wave asymmetry becomes more important than that of drift velocity, an expression for the equilibrium profile due to asymmetry, corresponding to Eq.(18), is then obtained as

$$h^5=\left(\frac{5.7\cdot\omega\cdot x}{\sigma^2}\right)^2 g. \tag{19}$$

Because the third term in the Eq. (16) would be canceled by the first and the second terms in the case of the above equilibrium profiles, if there exist another waves such as the long period waves as considered now, Eq. (9) would be reduced to a simple form of

$$\overline{i_s}=\frac{16\varepsilon_S\cdot C_D\cdot\rho}{3\pi\cdot\omega}u_{B1}\cdot u_0^3. \tag{20}$$

Equation (20) means that the net suspended load transport depends only on the drift velocity of long period waves in the equilibrium state. Saying it differently, the net transport due to the drift velocity of long period waves has an effect of sea bottom perturbation from the equilibrium profile.

Next, the drift velocity u_{B1} in Eq.(20) will be examined. The long period waves which have been detected quantitatively in the nearahore zone until now are considered to be either edge waves (e.g., *Huntley* and *Bowen* 1973, *Huntley* 1976 *Sasaki* and *Horikawa* 1978, *Holman* 1974, *Huntley* and *Bowen* 1978, *Huntley*, *Guza* and *Thornton* 1981, and *Katoh* 1981) or standing waves on a sloping beach (e.g., *Suhayda* 1974, and *Hotta*, *Mizuguchi* and *Isobe* 1981). The edge waves are three-dimensional waves, the surface elevation of which varies not only in the offshore direction but also in the longshore direction. The standing waves are two-dimensional waves, the surface of which varies only in the offshore direction. The on-offshore profiles of these waves, however, are hardly distinguished each other when a mode of edge waves is high. Since we are now studying on the multiple longshore bars of two-dimensional character, which are parallel to the shoreline, we examine the drift velocity due to standing waves on a sloping beach.

According to *Lamb* (1932), the wave profile and the velocity of standing waves on a sloping beach are

$$\zeta=C\cdot J_0(\xi)\cdot\cos\sigma_B t, \tag{21}$$

$$u_{B0}=C\frac{2\sigma_B}{\beta}\sin\sigma_B t\cdot\frac{J_1(\xi)}{\xi}, \tag{22}$$

$$\xi=\sqrt{x}\cdot\sqrt{\frac{4\sigma_B^2}{\beta}}, \tag{23}$$

where ζ is the displacement of the free surface from the static equilibrium position, C is a constant coefficient and represents the amplitude at the shoreline, ξ is a non-dimensional distance from the shoreline, and $J_0(\xi)$ and $J_1(\xi)$ are the zeroth and first order Bessel Functions of the first kind, respectively. In these expressions, the

horizontal and the vertical coordinates are increasing in the offshore direction and in the upward direction from zero at the shoreline and at the static water surface.

Bowen and *Inman* (1971) showed the drift velocity due to the standing waves of two horizontal dimensions, by using the result derived by *Hunt* and *Johns* (1963) for the drift velocity due to waves propagating in the two horizontal dimensions. Applying it to one horizontal dimension, we can reduce their result to

$$u_{B1}=-\frac{1}{2\sigma_B}\left(\overline{3u_{B0}\frac{du_{B0}}{dx}}\right). \tag{24}$$

By substituting Eq.(22) into Eq. (24) and integrating over the wave period, we have

$$u_{B1}=\frac{6C^2\cdot\sigma_B{}^3}{g\cdot\beta^3}\cdot\frac{\beta(\xi)}{\xi^3}, \tag{25}$$

where,

$$B(\xi)=-J_1(\xi)\{J_0(\xi)-\frac{2}{\xi}J_1(\xi)\}. \tag{26}$$

The function $B(\xi)$ is shown in Fig. 11 with the non-dimensional distance ξ from the shoreline. The profile of standing wave $J_0(\xi)$ is also shown in this figure with a scale reduced by factor of 5. The vertical coordinate is for the values of $B(\xi)$. As discussed previously with regard to Eq. (16), the direction of the net suspended load transport depends on a sign of u_{B1}, or $B(\xi)$ as seen in Eq. (25). At the areas where $B(\xi)>0$, the direction of the net transport of suspended load is offshore, and it is onshore where $B(\xi)<0$. Being judged from these properties, the directions of the net

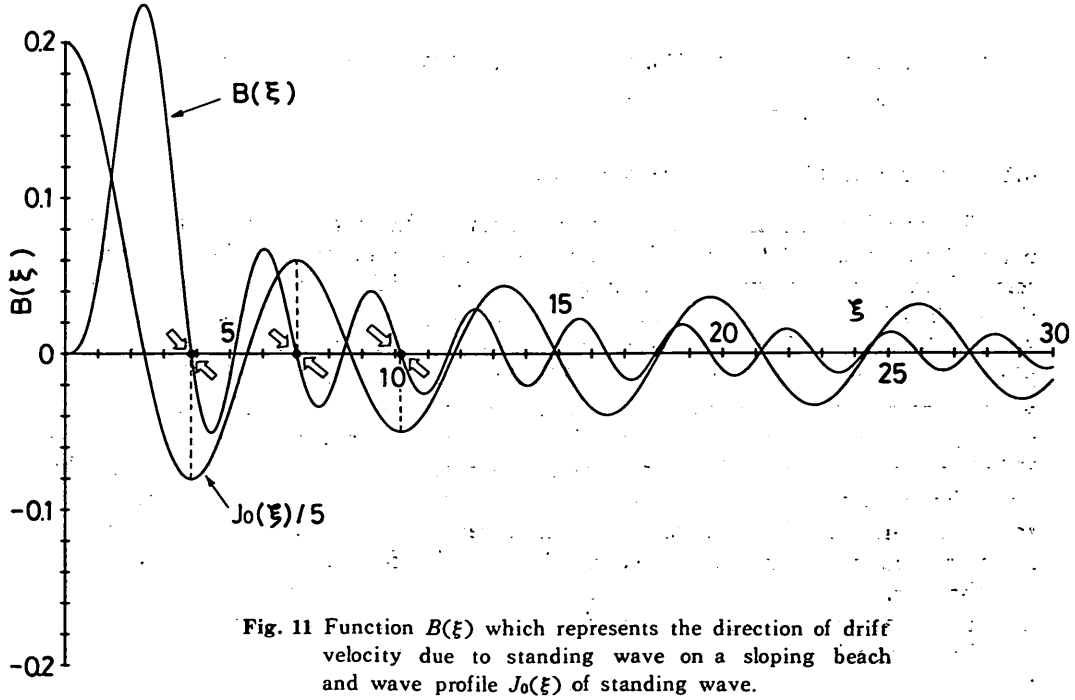

Fig. 11 Function $B(\xi)$ which represents the direction of drift velocity due to standing wave on a sloping beach and wave profile $J_0(\xi)$ of standing wave.

transport have been determined and shown with opened arrows in Fig. 11. The directions of the opened arrows and the profile of standing wave $J_0(\xi)$ show that the suspended sediments gather to the antinodes and deposit there, resulting in forming the longshore bars. That is to say, the locations of the bars are predicted by

$$J_0(\xi)=0, \tag{27}$$

where the values of ξ are readily obtained from any handbook of the tables of functions. They occur at

$$\xi=3.383,\ 7.016,\ 10.173,\ 13.324,\ \cdots\cdots, \tag{28}$$

or

$$\frac{4\sigma_B^2}{\beta}\cdot x=11.438,\ 49.224,\ 103.490,\ 177.530,\cdots\cdots. \tag{29}$$

The conclusion obtained in this section is superficially the same as those of the past theories (*Carter, Liu* and *Mei* 1973, *Bowen* 1980), in which only the standing waves reflected by the beach were taken into account. The implication of the present conclusion, however, is different from those of the past ones. In the past theories, the orbital velocity of standing waves must exceed the threshold velocity for the inception of sediment movement by a sufficient margin. On the other hand, the present conclusion means that the sediments which are suspended by the action of incident waves are transported by the drift velocity due to the long period waves of standing mode. Since the suspended sediments are easily transported by the flow of feeble velocity, longshore bars can be formed even if the orbital velocity of standing waves would be smaller than the threshold velocity.

4. Data Analysis of Multiple Longshore Bars and Long Period Waves at Hakui Beach

4.1 Features of Multiple Longshore Bars

The past location of multiple longshore bars in the area between the reference points No.29 and No.38 at Hakui Beach have been read from aerial photographs, some of which are shown in Photograph 1. The aerial photographs available are those taken in September 1963, September 1967, May 1968, June 1972 and May 1982. After adjusting the horizontal scale, they have been overlapped and are shown in Fig. 12. The figures on the foreshore in this figure are the numbers of reference points which correspond to those in Fig. 14, and the bars have been numbered, for convenience, from the offshore to the shoreline in the reverse order of the usual one. At Hakui Beach, the bars of four steps were usually formed on the sea bottom and they were almost parallel to the shoreline. The spacing between successive bars tended to increase in the offshore direstion. The distance of each bar from the shoreline, however, changed from year to year. For example, for the first bar, its location was the farthest in May 1968 and the nearest in September 1967 with the shifting distance of about 250 meters in the direction normal to the shoreline.

If the scale is normalized by dividing any distances by the distance from the fourth bar to the first one for each year's data, then a direct comparison can be

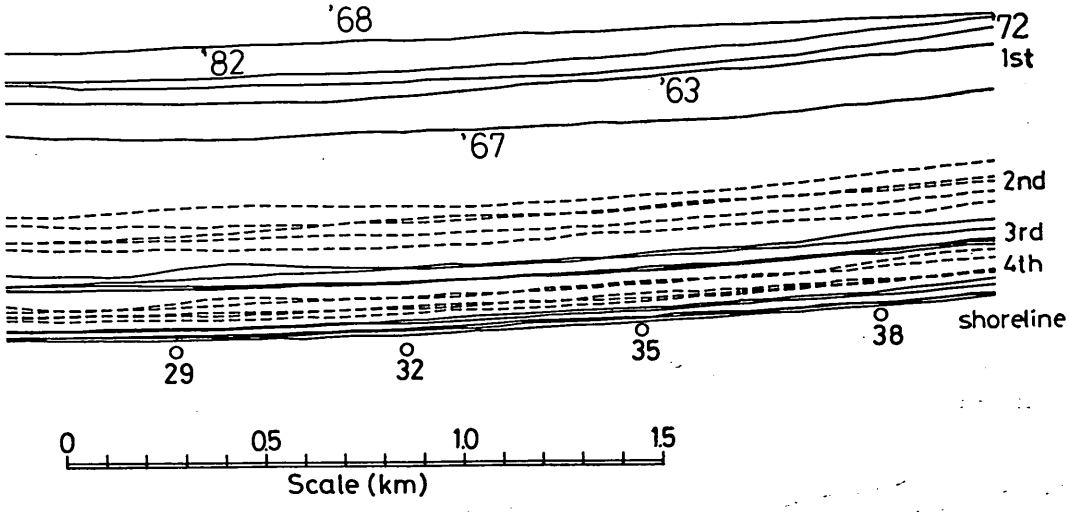

Fig. 12 Locations of multiple longshore bars in the area between reference point No. 29 and No.38 at Hakui Beach, which have been read from aerial photographs.

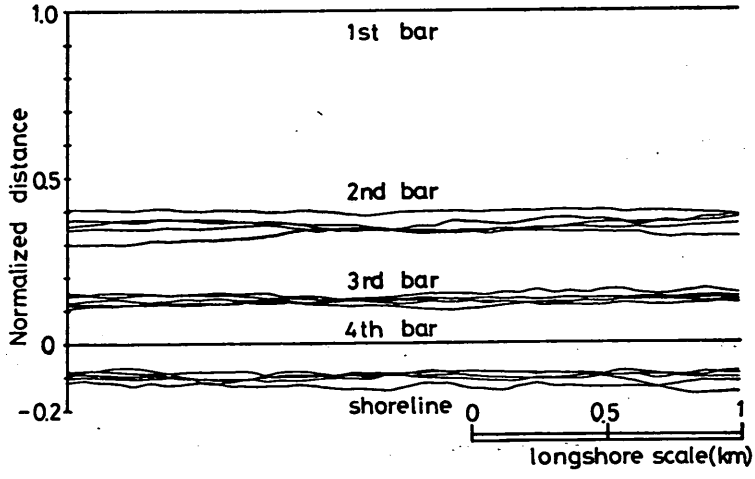

Fig. 13 Locations of multiple longshore bars which have been normalized by the distance from the fourth bar to the first bar of every year (in the area between reference point No.29 and No.38).

made with the theoretical predictions of Eqs. (27), (28) and (29). The reason why the distance from the shoreline to the first bar is not used for normalizing the scale is a difficulty in precisely locating the horizontal position of the shoreline in the aerial photographs. The result is shown in Fig. 13, in which we can recognize that the normalized distances are almost coincide with one another with the averaged values of -0.10 for the shoreline, of 0.13 for the second bar and of 0.36 for the third one. According to the theoretical results of Eq. (29), values corresponding to these normalized distances are -0.07, 0.23 and 0.55 respectively, which are

different from the actual values.

Before raising a question for the disagreement between the measured distances and theoretical ones of bar spacings, we must remember the assumption of a plane beach in the theory and must examine its applicability to the bottom profile at Hakui Beach. *Holman* and *Bowen* (1979) showed, by using a numerical model for edge waves wavelength on a real beach, that approximating a real beach profile by a single linear slope in some cases led to serious errors in estimating the dispersion relation for some values of edge waves' wavelength and frequency.

It is usually impossible to obtain the bottom profiles from the aerial photographs, although the locations of multiple longshore bars can be detected in them. Therefore, a contour map must be utilized for this purpose. The sea bottom topography at Hakui Beach was surveyed only once during the period of February to March in 1983, which is shown by a contour map in Fig. 14 (the locations of bars will be more clearly shown in Fig. 16). In this figure, we can recognize longshore bars of

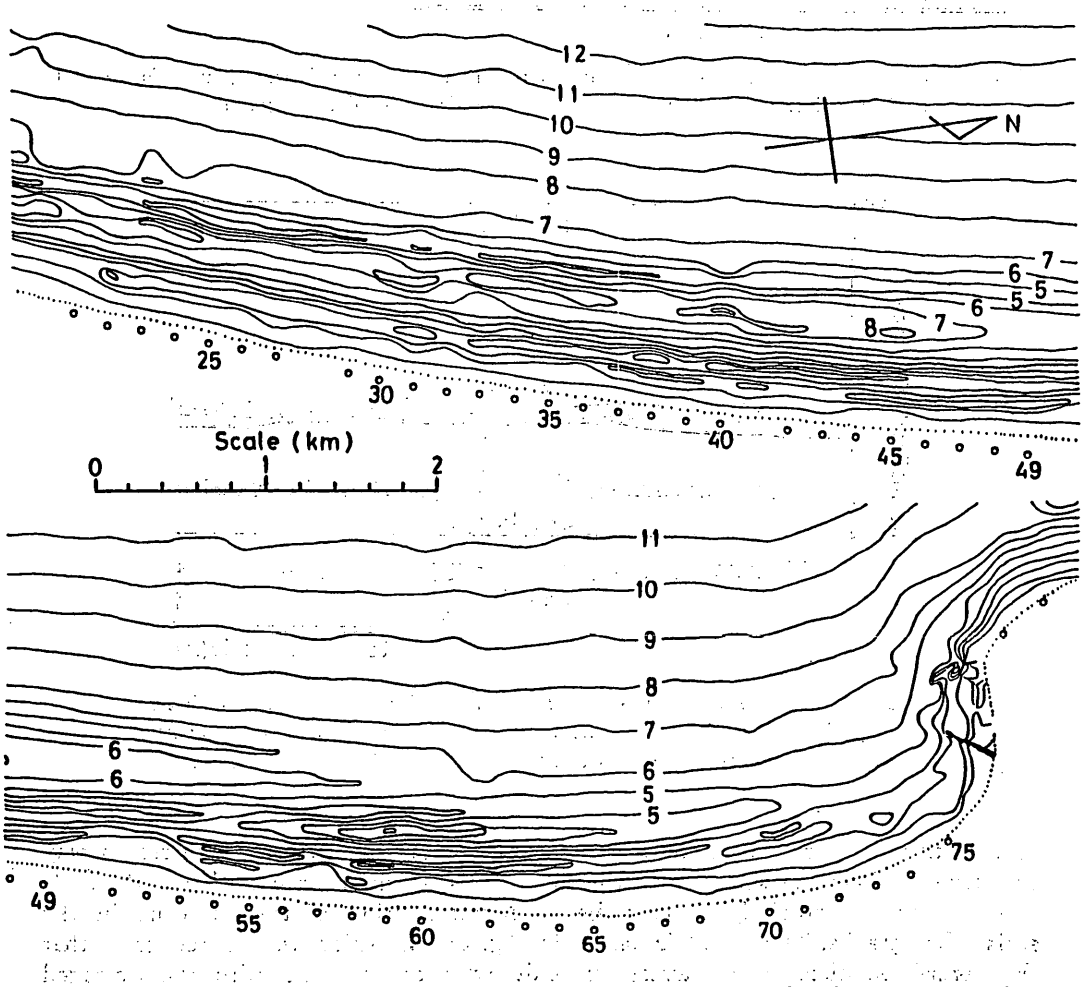

Fig. 14 Contour map at Hakui Beach, surveyed during the period of February to March, 1983 (with the courtesy of the prefectual government of Ishikawa).

three steps. However, the third bar, which is the nearest one to the shoreline, cannot usually be noticed in the longshore direction. The surveying might have been impossible to be completed, since it was located at the shallow water area and its size was the smallest. Otherwise it might have been locally swept away by the weak wave action after the storm conditions. A number of steps of bars was three in the contour map, while it was four in the aerial photographs. The surveying was done after the storm wave season, whereas all of the aerial photographs were taken in the calm wave season. Small scale bars might have been formed near the shoreline by mild waves in a calm season, superposing themselves on the bars formed previously in the storm conditions. Unfortunately, there is no more data available for examining this difference.

The beach profiles were surveyed along the measurement lines, which were normal to the shoreline passing through the reference points on the foreshore in Fig. 14. In order to roughly see the whole profiles at Hakui Beach, five groups of successive three profiles are shown by overlapping them for each group with dashed lines in Fig. 15. An interval of measurement lines was 200 meters and that of groups shown in Fig. 15 is about 2 kilometers in the longshore direction. The

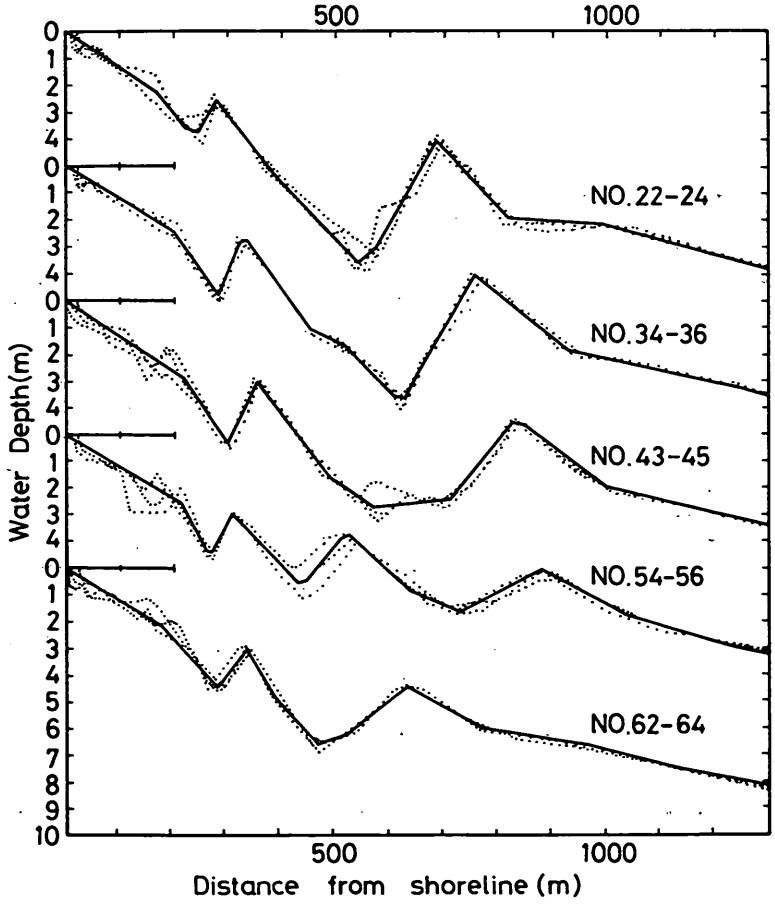

Fig. 15 Bottom profiles of five groups of successive three measurement lines.

successive three profiles in each group almost agree with one another and they can be represented by a broken solid lines as shown in Fig. 15. Each representative profile has two or three bars and troughs, which become larger in size in the offshore direction. Because of this character, the bottom profile is so complex that applying the assumption of a constant slope to this beach in the theoretical treatment may introduce some unacceptable error in the results. Especially at the deepest trough between the first and the second bars, the water depth is deep, which may result in prolongating the long period wavelength and shifting the position of antinodes of standing waves in the offshore direction.

Furthermore, except the group of No.62-64, the distances from the shoreline to the bars become larger and the mean bottom slope from the shoreline to the deepest trough becomes gradually gentler, as the location numbers of reference points in respective groups increase. In order to inspect the spatial distribution of the bars, the distances from the shoreline to the positions of the crests and troughs of bars have been read from the bottom profile along each measurement line ; the former are plotted with closed circles and the latter with opened circles respectively in Fig. 16. The first bar almost uniformly shifts from the location of 650 meters from the shoreline at the reference point No.19 to that of 890 meters at No.59, which are 8 kimometers apart in the longshore direction. However, it disappears in the area of right-hand

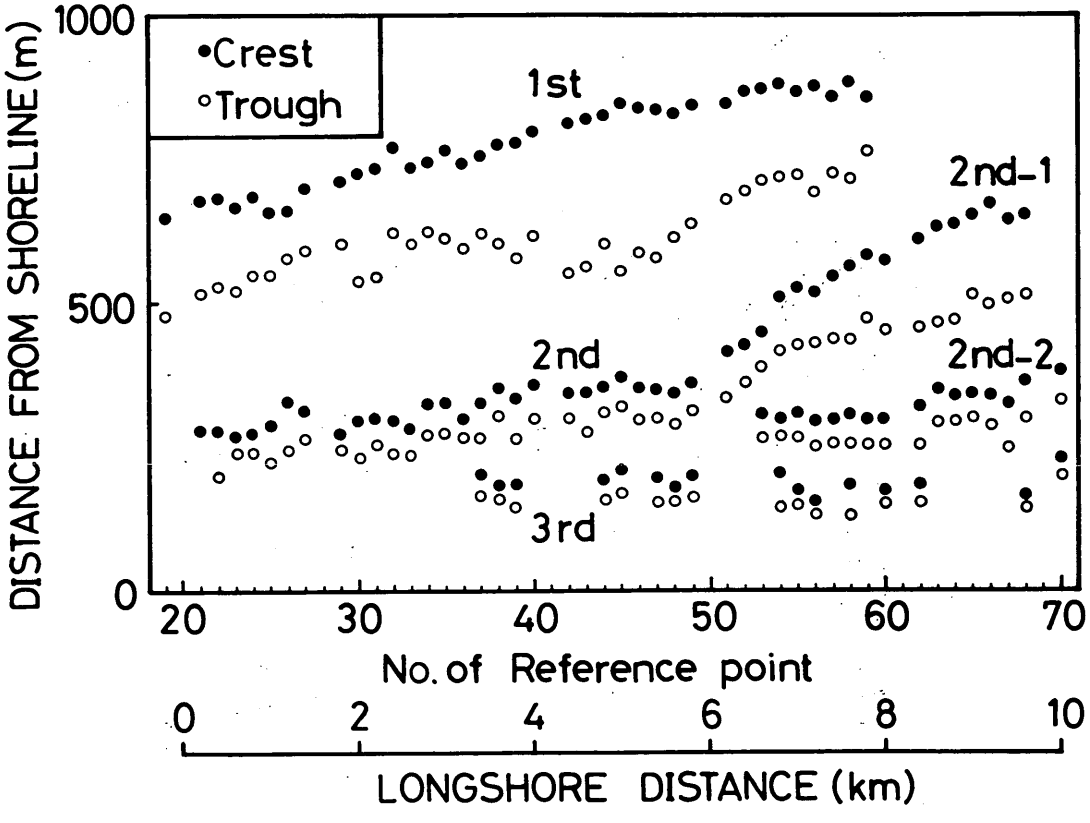

Fig. 16 Distances from the shoreline to the crests and troughs of longshore bars (surveyed during the period of February to march, 1983)

side from the reference point No. 59. The second bar also gradually shifts in the offshore direction and bifurcates at the reference point No. 50 as denoted by 2nd-1 and 2nd-2 in Fig. 16. From this point, the former rapidly shifts in the offshore direction, while the latter remains at the same location as the second bar of left-hand side of reference point No.50. Although the third bar existed continuously in the longshore direction in the aerial photographs, it is not always noticeable in the bottom profiles along the measurement lines.

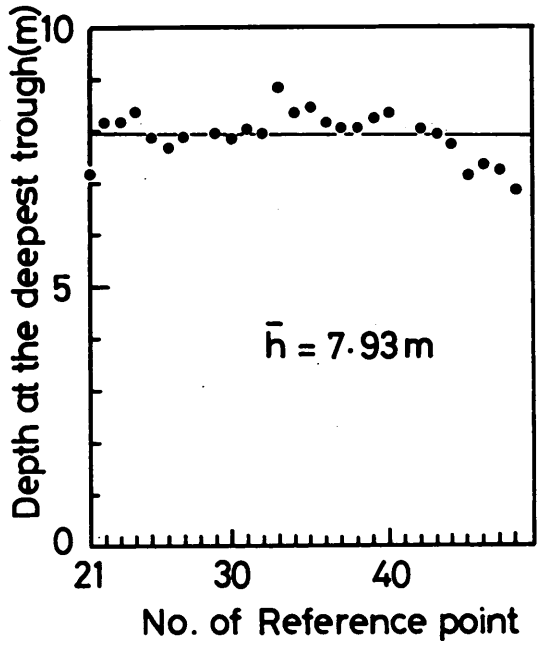

Fig. 17 Water depth of the bottom of the deepest trough on each measurement line (mean sea level of 0.16 meter above the datum line is taken into account).

The deepest trough between the first and the second bars also shifts in the offshore direction with the increase in the location number of reference point. Figure 17 shows the depth of the deepest trough for the area between the reference points No.21 and No.49. The depth is nearly constant, being about 8 meters in the mean value, from the reference points No. 21 to No.49, beyond wihch the trough becomes slightly shallower. By combining these two kinds of data, that is, the distance from the shoreline to the deepest trough and the water depth at the deepest trough, it becomes evident that the mean slope up to the deepest trough becomes gentler in the longshore direction as the location number increases; this change of the mean slope is further analyzed in Fig. 21. Since the bottom topography at Hakui Beach slightly changes in the longshore direction as described above, the assumption of a plane beach in the theoretical treatment might not be appropriate in this case.

Therefore, we need to calculate numerically the wave profile of long period waves on this non-constant sloping beach, which will be carried out in the next section.

4.2 Long Period Waves of Standing Mode on Complex Beach Profile

Since it is almost impossible to analytically obtain a solution for the long period waves on a complex beach profile, both the wave profile and the orbital velocity have been calculated by means of a digital computer by following the method by *Mizuguchi*, *Karibe* and *Hotta* (1983). Their method makes use of the theoretical solution of the long waves on a constant sloping beach.

The general two-dimensional solitions for the wave profile and the velocity of long waves on a constant sloping beach are

$$\zeta = a_i\{J_0(\xi)\cdot\cos\sigma_B t - Y_0(\xi)\cdot\sin\sigma_B t\} + 2a_r\cdot J_0(\xi)\cdot\cos\sigma_B t, \tag{30}$$

$$u_{B0} = \sqrt{\frac{g}{h}}\cdot[a_i\{J_1(\xi)\cdot\cos\sigma_B t + Y_1(\xi)\cdot\sin\sigma_B t\} + 2a_r\cdot J_1(\xi)\cdot\sin\sigma_B t], \tag{31}$$

where a_i and a_r are the amplitudes of incident waves and reflected wav esrespectively, J_0 and J_1 are the zeroth and first order Bessel functions of the first kind, and Y_0 and Y_1 are those of the second kind. In order to apply these equations to the complex beach profile, the beach profile must be approximated by a number of straight lines in advance as shown with solid lines in Fig. 15. By letting ζ and u_{B0} be continuous at the intersections of straight lines representing the bottom profile, the numerical solution can be obtained in the offshore direction from the first constant sloping area adjacent to the shoreline. For this purpose, a computer program developed by *Mizuguchi et al.*(1983) has been utilized, which was made possible by their courtesy.

Numerical calculations by means of a digital computer have been carried out for five representative profiles shown with broken solid lines in Fig. 15. Since the bars may be expected to be formed at the antinodes of standing waves as previously mentioned in Section **3. 2,** the locations of antinodes from the shoreline on these complex profiles have been examined on the basis of the results obtained. Figure 18 shows the relation between the frequency of long period waves and the locations of antinodes defined as the distances from the shoreline for five different profiles. From this figure, we can conclude that the relation between the long period wave frequency and the locations of bars is almost constant in spite of the differences in the bottom profiles. This result suggests that the bars formed on the sea bottom, the location of which are different from a group to another group as seen in Fig. 15, influence the dispersion relation of standing waves only slightly. *Kirby*, *Dalrymple* and *Liu*(1981) developed a numerical model to calculate the profiles and wavelengths of edge waves for arbitrary bottom profiles and a given frequency. Applying their model to the case of a beach with multiple longshore bars, they found that the bars had no effect on the dispersion relation of edge waves.

By utilizing Fig.16 and the mean curve for the location of the first antinode in Fig. 18, we can determine for each representative bottom profile the frequency of long period waves which has the antinode at the same location as that of the first bar on the bottom profile. This frequency is called the prevailing frequency of the long period waves in the following discussions. Figures 19 (a)-(e) show the bottom profiles and the spatial variation of the orbital velocity amplitude of the long period waves of standing mode with the prevailing frequency thus determined for the five representative groups of bottom profiles. As seen in these figures, the locations of the first and second bars well agree with those of antinodes of the wave profiles, or the

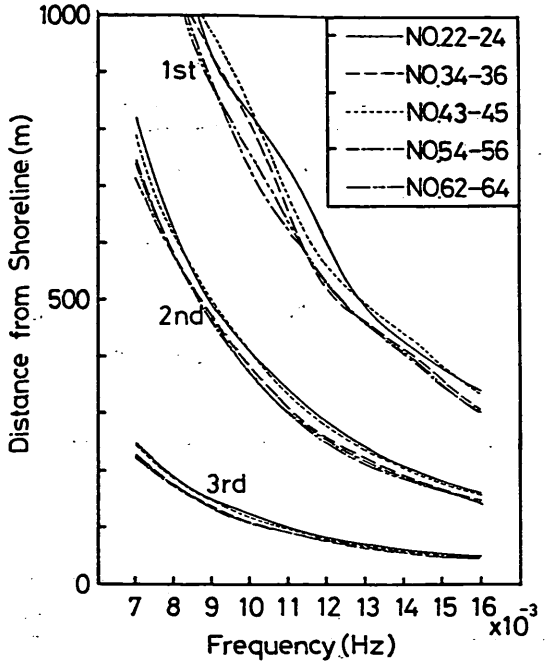

Fig. 18 Theoretical relation between the frequency of long period waves and the locations of the antinodes of their standing waves for five representative profiles shown in Fig 15.

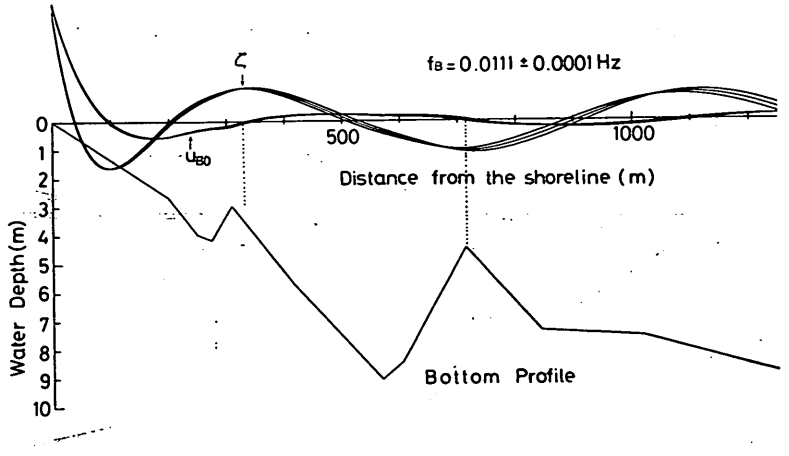

Fig. 19 (a) Representative cross section of measurement lines through No.22 to 24.

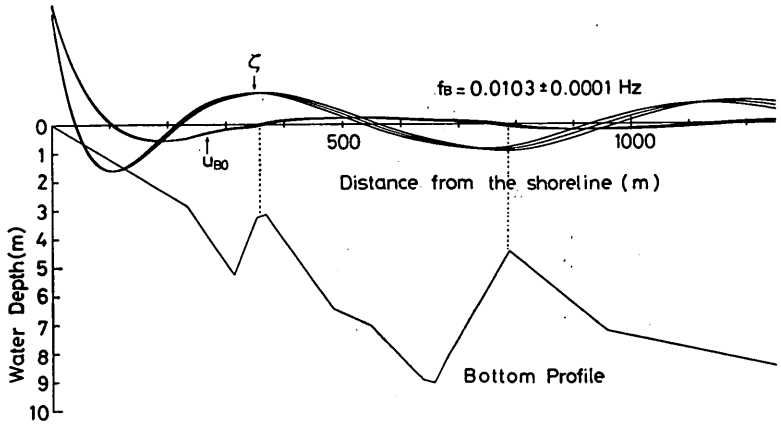

Fig. 19 (b) Representative cross section of measurement lines through No.34 to 36.

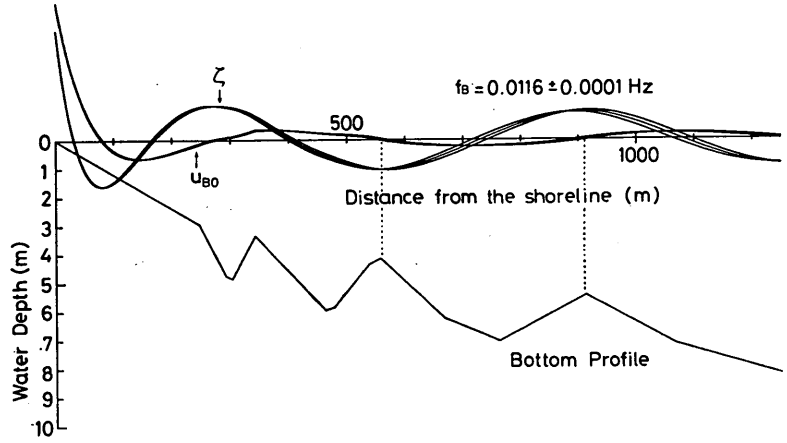

Fig. 19 (c) Representative cross section of measurement lines through No. 43 to 45.

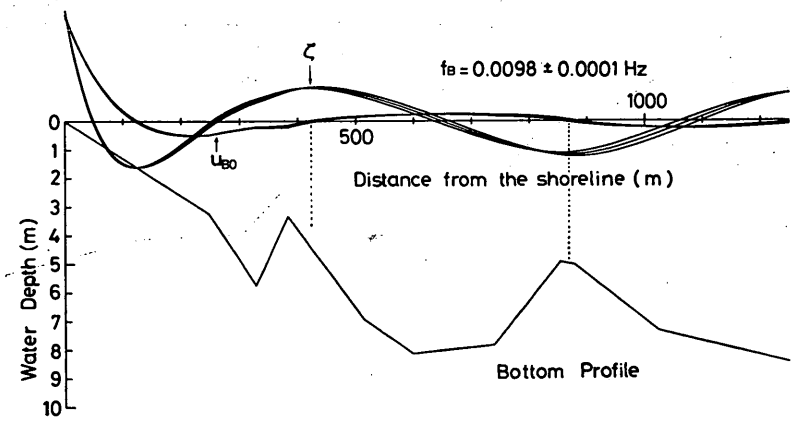

Fig. 19 (d) Representative cross section of measurement lines through No.54 to 56.

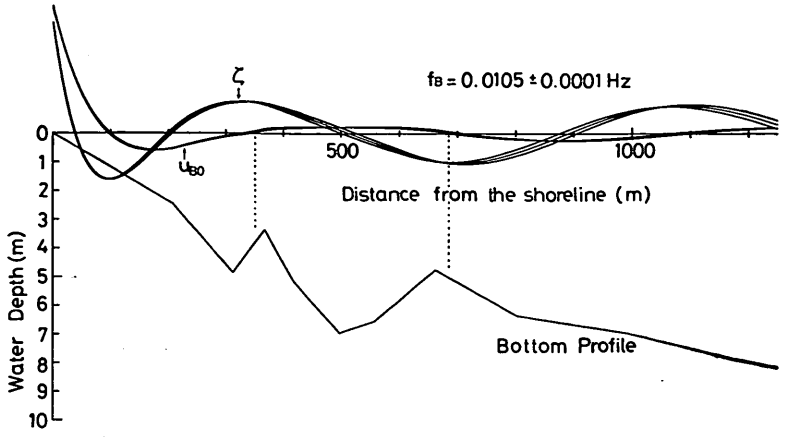

Fig. 19 (e) Representative cross section of measurementlines through No 62 to 64.

Fig. 19 Profiles and velocity amplitudes of long period waves of standing mode on complex beach profiles shown in Fig 15.

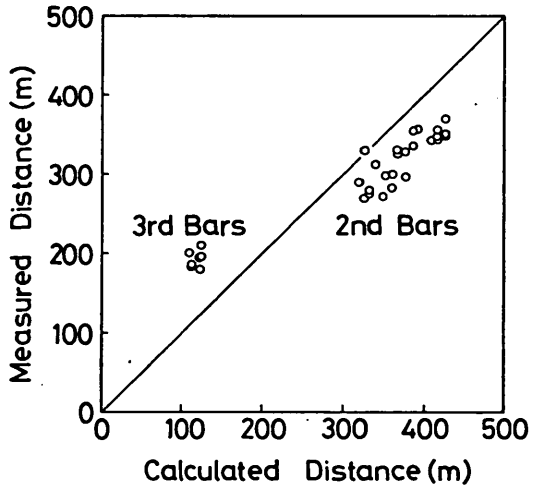

Fig. 20 Comparision of predicted locations and actual locations of the second and the third bars.

nodes of wave velocities in every group.

The prevailing frequency of the long period waves has also been determined along each measurement line between the reference point No. 21 and No.48 shown in Fig.16. With this data of wave frequency for the location of the first bar, prediction was made for the location of antinodes of the standing waves corresponding to the second and the third bars on the basis of Fig. 18. Figure 20 shows the comparison of the calculated results with the measured results. In this figure the horizontal axis represents the calculated distances from the shoreline to the locations of antinodes of the standing waves, while the vertical axis is the measured distances to the locations of bars which are read from Fig.16. The straight line indicates that the calculated

and the measured results agree with each other on it. The results for the first bars, whose distances from the shoreline are about 650 to 850 meters, are not shown in this figure. That is because the frequency of long period waves has been so determined that the calculated distance of the first bar would be in agreement with the measured one. As seen in Fig. 20, all the data are plotted near the straight line, even though the data shows a tendency that the calculated results are about 50 meters larger for the second bars, and about 70 meters smaller for the third bars than the measured ones.

4.3 Relationship between Beach Slopes and Frequencies of Long Period Waves

Since the location of bar gradually shifts in the offshore direction with the increase in the location number in the longshore direction, the prevailing frequency of long period waves determined in the manner described in Section 4.2 are different from one measurement line to another. In this section, the cause for this difference will be examined for the measurement lines between No. 21 and No. 48, where the trend of changes in the frequency and that in the bar location are almost constant.

The prevailing frequency of long period waves for each measurement line is shown with opened circle in Fig. 21. The prevailing frequency linearly decreases with the increase in the location number of reference point in the longshore direction. The average of the prevailing frequencies is about 0.0105 Hz which almost corre-

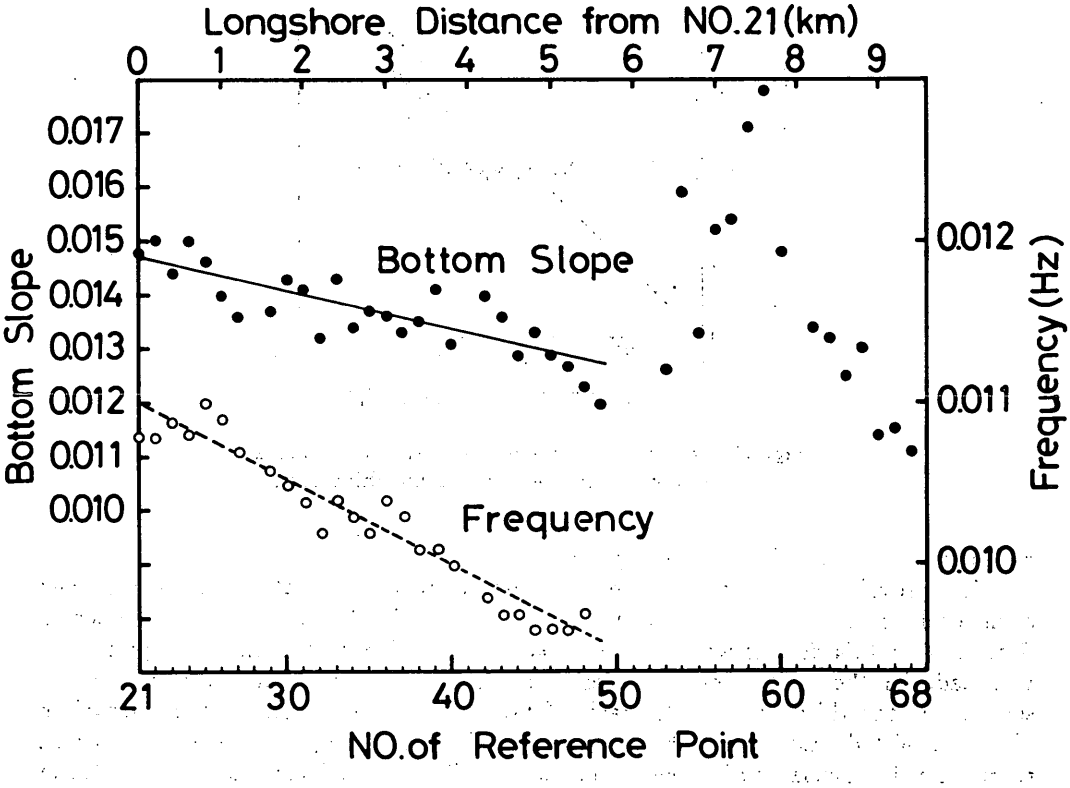

Fig. 21 Prevailing frequency of long period waves which has been determined by utilizing Fig. 16 and 18, and the mean bottom slopes from shoreline to the deepest trough.

sponds to the second energy peak frequency in the averaged apectral densities of 505 records (see Fig.5). By means of the least square method, the decreasing tendency of frequency can be expressed as

$$f_B = -2.66\times10^{-4}\cdot y + 1.11\times10^{-2} \text{ (Hz)}, \tag{32}$$

where f_B is the prevailing frequenncy of long period waves in Hz and y is the longshore distance in kilometers from the reference point No. 21. Equation (32) is shown with a dashed line in Fig. 21.

The mean bottom slope from the shoreline to the deepest trough (see Fig. 15) on each measurement line is also plotted with closed circle in Fig. 21. It can be recognized that the mean bottom slope also has a tendency of decreasing from the reference point No.21 to No.49, although there is some scatter of data around the solid line, which has been obtained by the least square method as

$$\beta = -3.51\times10^{-4}\cdot y + 1.47\times10^{-2}, \tag{33}$$

where β is the mean bottom slope and y is the longshore distance in kilometers from the reference point No. 21.

By eliminating the term of y from Eqs.(32) and (33), we have

$$\beta = 1.32\cdot(f_B + 1.4\times10^{-4}). \tag{34}$$

Since the value of f_B is in the order of 0.01Hz, the constant value of 1.4×10^{-4} is negligible comparing with f_B. Therefore, we have

$$\beta/f_B = 1.32 \tag{35}$$

as an approximate relationship between the bottom slope and the prevailing frequency of long period waves whose antinodes agree with the bars in location.

By expressing wave motions in the Lagragian description, *Shuto*(1972) theoretically analyzed the behaviour of long waves on a somewhat complex beach having a constant slope connected to a uniform depth in the offshore, and he obtained a breaking condition of the incident long waves on the slope as follows :

$$H_{BC} = \frac{g}{2\pi^2}\left(\frac{\beta}{f_B}\right)^2 (J_0^2(x) + J_1^2(x))^{1/2}, \tag{36}$$

where,

$$x = 4\pi\left(\frac{f_B}{\beta}\right)\sqrt{\frac{h_H}{g}}, \tag{37}$$

H_{BC} and f_B are the wave height and the frequency of reflected standing waves respectively, β is the beach slope of sloping section, h_H is the water depth at the section of uniform depth and g is the acceleration of gravity. By substituting Eq. (35) into Eqs.(36) and (37), we have

$$H_{BC} = 0.865(J_0^2(x) + J_1^2(x))^{1/2}, \tag{38}$$

where,

$$x = 3.041\sqrt{h_H}. \tag{39}$$

Figure 22 shows the relation between H_{BC} and h_H based on Eqs. (38) and (39).

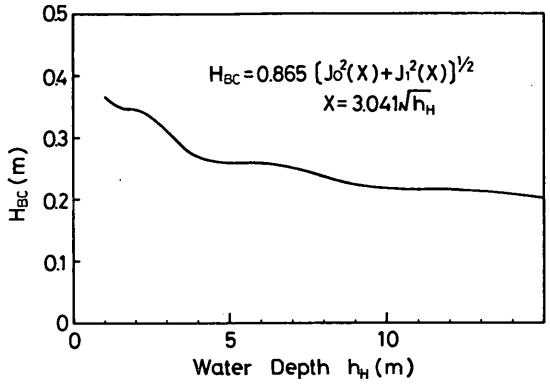

Fig. 22 Relation between critical wave height of long wave breaking and water depth in horizontal bottom.

Before applying this result to the bottom profile of Hakui Beach, the following questions have been considered for how to determine the horizontal depth h_H. According to Fig.17, the depth of the deepest trough, to which location the mean beach slope β has been defined from the shoreline along each measurement line, is slightly scattered around the mean depth of about 8 meters. Since the first bar exists at the offshore side of this trough, it is open to question whether it is proper or not to use 8 meters for the horizontal depth h_H in Eq. (39). The critical breaking height H_{BC}, however, is almost independent of the depth of uniform section beyond about 8 meters as seen in Fig.22. Therefore, by setting $h_H=8$ meters, we have from Fig.22

$$H_{BC}=0.23 \text{ (meter)}. \tag{40}$$

Next, the height of long period waves at the depth of 8 meters will be estimated on the basis of the actual wave data of Hakui Beach. From Eq.(3), the ratio of the wave height of long period waves at the depth of 8 meters (H_{B8}) to that of 20.16 meters (H_{B20}) is obtained as

$$\frac{(\zeta_{rms})_8}{(\zeta_{rms})_{20}}=\frac{H_{B8}}{H_{B20}}=\sqrt{\frac{H_S+20.16}{H_S+8}}, \tag{41}$$

where the change of incident wave height due to wave shoaling is ignored as negligible in the derivation. As mentioned in Section **2.3** (see Fig.9), the long period waves of 0.16 meter in height occurred most frequntly at the depth of 20.16 meters when the significant wave height of incident waves was exceeding 2 meters. Then, by substituting $H_{B20}=0.16$ meter at the depth of 20.16 meters and $H_S=2\sim4$ meters into Eq.(41), we ultimately have the relation of

$$H_{B8}=(1.42\sim1.49)\cdot H_{B20}=0.23\sim0.24 \text{ meter}. \tag{42}$$

From Eqs.(40) and (42), it can be concluded that the critical breaking height H_{BC} is almost equal to the modal height of long period waves at the depth of 8 meters. That is to say, at Hakui Beach a set of the conditions for the mean bottom slope β , the prevailing frequency of long period waves f_B, and the modal height of

splong period waves at the depth of 8 meters H_{B8} satisfies Eqs. (36) and (37), which are the critical condition of long wave breaking on a sloping beach derived theoretically by *Shuto* (1972). Therefore, the long period waves with the modal height and the frequency greater than the prevailing values must have been broken at the shore of Hakui Beach, while the long period waves with the frequency less than the prevailing values must have been reflected from the shore without breaking.

4.4 Discussions on the Result of Data Analysis

The locations of bars in the right-hand area from the reference point No.50 will be examined. In this area, the bottom slope, which is defined from the shoreline to the trough between the bars of 2nd-1 and 2nd-2 in Fig.16, is the steepest at the reference point No.58 as seen in Fig.21. From this point to the direction to the right, it becomes gentle rapidly. At Hakui Beach, Eq. (35) of the relationship between the bottom slope and the prevailing frequency is a necessary condition to satisfy breaking condition of the long period waves (Eq.36) if we assume the uniformity of the long period wave height in the longshore direction. According to Eq. (35), the decrease of the beach slope is associated with the decrease in the prevailing frequency of long waves, which in turn elongates the wave length, or makes the locations of bars far away from the shoreline. Therefore, it is said that the rapid decrease of the bottom slope from the reference point No. 58 to the rightward direction corresponds to the rapid shifting of the bar to the offshore direction, as denoted by 2nd-1 in Fig.16. In the area between the reference point No. 53 and No.59, the bars of four steps were formed as seen in Fig.16. This area is considered to have been the transition zone from the left to the right beach or vice versa.

There is one comment on the difference of bar steps between in the aerial photographs and in the contour map. As we know, in the calm season the sand is accumulated on the foreshore and the beach slope near the shoreline becomes steep, whereas in the storm season the foreshore is eroded and the beach slope becomes gentle. That is to say, the critical frequency of breaking becomes high (or short period) in the calm season and low (or long period) in the storm season. Therefore, if the storm waves will happen to come in the calm season, the bars having the short spacing would be frormed. This might have been one reason for the existence of the bars of four steps in summer.

Kirby, Dalrymple and *Liu*(1981) concluded, after calulating the features of the edge waves on a beach with multiple longshore bars by utilizing their numerical model, that the longshore bars have a function of trapping the antinodes of the wave profiles at the bar locations. Their result shows a possibility that a beach profile with well-developed bars has the ability to modify the profiles of standing edge waves in a manner leading to self-maintenance, although they did not explain the resonance phenomena of the edge waves since wave amplitudes were calculated in normalized form. *Symonds, Huntley* and *Bowen*(1982) developed a theory of two-dimensional setup within the surf zone with a time-varying breakpoint of the incident waves and showed that the time variation of the breakpoint, which occurs when the incident waves are of varying amplitude, can generate waves at the group period and may be a significant source of long wave energy. By applying this theory to the beach with a shore parallel bar, *Symonds* and *Bowen*(1984) have recently explained skillfully two possible resonance conditions of standing waves between the shoreline and the mean breakpoint over the bar. One is a quarter wavelength resonance condition, having a node of the surface elevation of long period waves over the bar. Another is a half

wavelength resonace, having a antinode over the bar. According to their result, at resonance the constructive modes of the half wavelength condition, those tending to maintain the bar, are amplified, while the destructive modes of the quarter wavelength condition, those tending to create a trough at the bar position, are actually suppressed by the topography. In the theories of *Kirby et al.* (1981) and *Symonds et al.*(1984), they assumed the long period waves were reflected completely from the beach. As examined in the previous section, the long period waves with the frequency less than the prevailing values at Hakui Beach were reflected without breaking. These long period waves must have acted as the half wavelength resonator in amplifying the system of multiple longshore bars.

According to the theoretical solution of *Carter*, *Liu* and *Mei* (1973), when the reflection coefficient R is smaller than 0.414, the direction of drift velocity u_{B1} due to the partial standing waves is as same as that of the incident waves in the whole area. As a result, the bars should not be formed when the reflection coefficient is small. *Bowen* (1980) predicted that the longshore bars will be developed in large size by the standing waves having a high reflection coefficient. By taking these previous studies into account, the multiple longshore bars may be obscure or disappeared in shape under the action of the partial standing waves.

Since the long period waves with the frequency greater than the prevailing values were breaking at Hakui Beach, they were incapable of forming the multiple longshore bars. The long period waves which formed the bars at Hakui Beach must have had the frequency equal to or less than the prevailing values at respective locations. The drift velocity due to the perfect standing waves, which has an important role to transport the bed materials and to form the bars, is proportional to the third power of the wave frequency as seen in Eq. (25) ($B(\xi)/\xi^3$ represents the non-dimensional feature of the drift velocity.). Thus, the power of the long period waves in forming the bars rapidly decreases with the decrease in the frequency, even if the wave height dose not change. Therefore, the long period waves having the prevailing frequencies must have exercised the largest effect among the waves of various frequencies on the formation of the multple longshore bars, and thus the locations of the bars must have been governed by the prevailing frequencies of long period waves.

There is another evidence that suggests simultaneous actions of long period waves with various frequencies in the fromation of longshore bars. In the typical aerial photographs in Photograph 1, we can detect the locations of multiple longshore bars based on a contrast by the bright tone of shallow bar crests against the dark background of deep troughs. If examined in more detail, the color of photographs distinctly changes from the dark background to the bright tone at the locations of bar crests in the offshore direction, and then the bright tone gradually diminishes to the dark tone. These changes in color indicate a rapid rise of the sea bottom from a trough toward the next offshore bar crest and a gradual fall from a bar crest toward the next offshore trough. Such a bathymetric feature can also be noticed in the bottom profiles in Fig.15. If the longshore bars are formed by the long period waves having the frequency up to the prevailing frequencies, the locations of the antinodes of standing waves of respective frequencies are aligned in the offshore direction from that of the prevailing frequencies toward those of lower frequencies because the wavelength increases in that order. Since the long period waves with the greatest frequencies, that is, the prevailing frequencies, exercise the largest effect in the formation of longshore bars, the onshore slope of a bar should be rather steep and the offshore slope should be rather gentle. This is in agreement with the evidence

in the aerial photographs and the bathymetry.

After being formed on the sea bottom as mentioned above at an initial stage, the bars in turn may be amplified by the mechanism of a positive feedback system due to the half wavelength resonance of the long period waves predicted by *Symonds* and *Bowen*(1984). According to their theory (Eq. 22 in their paper), the frequency of half wavelength resonator mainly depends on the dimensions in the onshore-side area of the bars, that is, the distance from the shoreline to the bar and the depth between the shoreline and the bar. The long period waves with the prevailing frequencies also depend on these dimensions at the initial stage.

This result can be interpreted in such a way that the multiple longshore bars at Hakui Beach must have been formed and amplified by the perfectly reflected long period waves with the prevailing frequencies.

5. Conclusions

In order to give satisfactory explanation for the origin of the multiple longshore bars, a theory is developed and the actual data of the bottom topography and the waves at Hakui Beach in Japan are analyzed. The main conclusions obtained in this paper are as follows :

(1) By examining the aerial photographs along the coast lines of Japan, the most typical example of two-dimensional multiple longshore bars was found out as those at Hakui Beach in Japan.

(2) The long waves of about 100 seconds in period coexist with the incident wind waves at Hakui Beach. The ratio of the significant wave height of long period waves to that of incident waves satisfies *Goda's* empirical equation.

(3) It is inferred that the suspended load transport must be more significant than the bed load transport in the storm wave conditions at Hakui Beach.

(4) By following the approach by Bowen(1980), an expression for the net transport rate of suspended load under the action of both the incident waves and the long period waves of standing mode is derived as Eq.(16). Based on this equation, it is shown that the sediments suspended by the action of incident waves are transported by the drift velocity due to the long period waves of standing mode, resulting in the formation of the multiple longshore bars.

(5) The locations of bars well agree with those of antinodes of the standing waves of about 0.01 Hz in frequency, which are corresponding to the energy peak frequency in the averaged wave spectral density at Hakui Beach.

(6) The actual conditions of the mean bottom slope, the prevailing frequency of long period waves and the wave height of long period waves at the depth of 8 meters satisfies *Shuto's* equations of the critical condition of long wave breaking on a sloping beach.

(7) The multiple longshore bars at Hakui Beach have been formed and amplified by the existence of the perfectly reflected long period waves with the prevailing frequencies.

Since the long waves of 1 to 3 minutes in period have very small wave steepness, they should be perfectly reflected by a natural beach and artificial structures. Then, there should exist the long period standing waves of complex modes around the structures, such as detached breakwaters, jetties and breakwaters, which should

play a important role to deform the bottom topography. Therefore, the result of this paper will give a new viewpoint for understanding the deformation of bottom topographies around the structures in the nearshore zone.

Acknowledgement

The author is grateful to Dr. Yoshimi Goda, the Director of the the Hydraulic Engineering Division, for helpful suggstions and observation and his critical reading of the manuscript. The author is also grateful to Dr. Masaru Mizuguchi for his courtesy for using a computer program of long period waves on a complex beach profile. Mr. Sei-ichi Himoto, a coastal engineer of the prefectual government of Ishikawa, who has been in Hakui from his childhood gave the author valuable information on Hakui Beach. The author received earnest assistances from Mrs. Keiko Tanaka in sorting a great number of aerial photographs. The author also should like to express his grateful thanks to the prefectual government of Ishikawa for making available him of contour maps at Hakui Beach and to the First District Construction Bureau, Ministry of Transport, and the Coastal Observation Laboratory, Port and Harbour Research Institute, for utilizing the wave data of Kanazawa Port.

(Received on June 30, 1984)

References

1) BAGNOLD, R. A. (1962) : Autosuspension of transported sediment ; Turbidity Currents, *Proc. of the Royal Society of London, Series A*, Vol.265, pp.315-319.
2) BAGNOLD, R.A. (1963) : Mechanics of marine sedimentation, *in the Sea*, Vol. 3, edited by M. H.Hill, Intersience, pp. 507-528.
3) BARUSSEAU, J. P. and B. SAINT-GUILY (1981) : Distribution, characteristics and formation of crescentic bars in the Gulf of Lions, *Oceanologica*, Vol 4, No 3, pp. 297-304. (in French).
4) BOWEN, A.J. and D.L. INMAN (1971) : Edge waves and crescentic bars, *J. Geophy. R.*, Vol.76, No.36, pp.8662-8671.
5) BOWEN, A. J. (1980) : Simple models of nearshore sedimentation ; Beach profile and longshore bars, *in the Coastline of Canada*, Edited by McCann, S.B., Geological Survey of Canada, Ottawa, pp.1-11.
6) CARTER, T.G., P.L-F.LIU and C.C.MEI (1973) : Mass transport by waves and offshore sand bedforms, *American Society of Civil Engineers, Journal of Waterways, Harbors, and Coastal Engineering Division*, WW2, pp.165-184.
7) DAVIS, R.A., Jr (1978) : Beach and nearshore zone, *Coastal Sedimentary Environments*, Edited by Davis, R.A., Springer-Velag, New York, pp.237-285.
8) GODA, Y.(1975) : Deformation of irregular waves due to depth-controlled wave breaking, *Report of the Port and Harbour Research Institute*, Ministry of Transport, Japan, Vol.14, No.3, pp.59-106. (in Japanese), or (1975) *Coastal Eng. in Japan*, JSCE, Vol.18, pp.13-26.
9) GODA, Y. (1979) : A review on statistical interpretation of wave data, *Report of the Port and Harbour Research Institute*, Ministry of Transport, Japan, Vol.18, No.1, pp.5-32.
10) HOLMAN, R.A., D.A. HUNTLEY and A.J. BOWEN (1974) : Infragravity waves in storm conditions, *Proc. 16th Int. Conf. on Coastal Eng.*, pp. 268-284.
11) HOLMAN, R.A. and A.J. BOWEN (1979) : Edge waves on complex beach profiles, *J.Geophy. R.*, Vol.84, No.C10, pp.6339-6346.
12) HOLMAN, R.A.(1981) : Infragravity energy in the surf zone, *J. Geophy. R.*, Vol.86, No. C7, pp.6442-6450.
13) HOLMAN, R.A. and A.J.BOWEN (1982) : Bars, bumps, and holes : Models for the genera-

tion of complex beach topography, *J. Geophy. R.*, Vol.87, No.C1, pp.457-468.

14) HOM-MA, M. and C.SONU (1962) : Rhythmic pattern on longshore bars related to sediment characteristic, *Proc. 8th Int. Conf. on Coastal Eng.*, pp.248-279.

15) HOTTA, S., M. MIZUGUCHI and M. ISOBE (1981) : Observations of long period waves in the nearshore zone, *Coastal Eng. in Japan*, JSCE, Vol.24, pp.41-76.

16) HUNT, J. N. and B. JOHNS (1963) : Currents induced by tides and gravity waves, *Tellus*, Vol.15, No.4, pp.343-351.

17) HUNTLEY, D.A and A.J. BOWEN (1973) : Field observation of edge waves, *Nature*, Vol. 203, No. 5403, pp.160-162.

18) HUNTLEY, D.A. (1976) : Long-period waves on a natural beach, *J. Geophy. R.*, Vol.81, No.36, pp.6441-6449.

19) HUNTLEY, D.A. and A.J. BOWEN (1978) : Beach cusps and edge waves, *Proc. 16th Int. Conf. on Coastal Eng.*, pp.1378-1393.

20) HUNTLEY, D.A.,R.T. GUZA and E.B. THORNTON (1981) : Field odservations of surf beat, 1. Progressive edge waves, *J. Geophy. R.*, Vol.86, No.C7, pp.6451-6466.

21) IRIE, I., K. NADAOKA, T.KONDO and K. TERASAKI (1984) : Two dimensional seabed scour in front of breakwater by standing waves, - A study from the standpoint of bedload movement -, *Report of the Port and Harbour Research Institute*, Vol.23, No. 1, pp.3-52 (in Japanese), or(1984) *Proc. 19th Int. Conf. on Coastal Eng.* (in preparing).

22) KATOH, K.(1981) : Analysis of edge waves by means of empirical eigenfunction, *Report of the Port and Harbour Research Institute*, Ministry of Transport, Japan, Vol.20, No. 3, pp.3-51.

23) KIRBY, J.T., R.A. DALRYMPLE and P.L.-F. LIU (1981) : Modification of edge wave by barred-beach topography, *Coastal Eng.*, Vol.5, No.1, pp.35-49.

24) LAMB, H.(1932) : Hydrodynamics, 6th ed., Art.185, Dover, New York, 738p.

25) LAU, J. and B.TRAVIS(1973) : Slowly varying Stokes Waves and submarine longshore bars, *J. Geophy. Res* , Vol.78, No.21, pp. 4489-4497.

26) MIZUGUCHI, M.(1979) : Edge waves in the field of Coastal Engineering, *Proc. of 15 th summer seminor on Hydraulics*, course B-4, JSCE, 20p.(in Japanese).

27) MIZUGUCHI, M., Y. KARIBE and S. HOTTA (1983) : On run-up waves on beaches in the field, *Proc. 30th Japanese Conf . on Coastal Eng.*, Vol.15, pp.13-23.(in Japanese).

28) MUNK, W.H.(1949) : Surf beats, *Trans. A.G.U.*, Vol.30, No.6, pp.849-854.

29) MUNK, W.H.(1962) : Long ocean waves, Chapter 18 of *the Sea* edited by M.H. Hill, Vol. 1, Intersience Pub., pp.647-663.

30) OZASA, H.(1977) : Resent shoreline changes in Japan, - An investigation using aerial photographs -, *Coastal Eng. in Japan*, JSCE, Vol.20, pp.69-81.

31) SASAKI, T. and K. HORIKAWA (1978) : Observation of nearshore current and edge waves, *Proc. 16th Int. Conf. on Coastal Eng.*, pp.791-809.

32) SHI-LENG, X.(1981) : Scouring patterns in front of vertical breakwaters and their influence on the stability of the foundations of the breakwaters, *Technische Hogeschool*, Delft (Netherlands), 61p.

33) SHOET, A.D.(1975) : Multiple offshore bars and standing waves, *J. Geophy. Res.*, Vol.80, No.27, pp.3838-3840.

34) SHORT, A.D. and P.A.HESP(1982) : Wave, beach and dune interactions in Southeastern Australia, *Marine Geology*, 48, pp.259-284.

35) SONU, C.J.(1968) : Collective movement of sediment in littoral environment, *Proc. 11th Int. Conf. on Coastal Eng.*, pp.373-400.

36) SONU, C.J.(1972) : Comments on paper by A.J. BOWEN and D.L. INMAN, "Edge waves and crescentic bars", *J. Geophy. R.*, Vol.77, No.33, pp.6629-6633.

37) SUHAYDA. J, N.(1974) : Standing waves on beachs, *J. Geophy. Res.*, Vol.79, No. 21, pp. 3065-3071.

38) SUHAYDA, J.N.(1975) : Determining infragravity wave spectra, *Int. Symp. Ocean Wave Meas. Anual.*, 1, pp.54-63.

39) SYMONDS, G., D.A.HUNTLEY and A. J. BOWEN(1982) : Two-dimensional surf beat ; Long

wave generation by a time-varying breakpoint, *J. Geophy. Res.*, Vol. 87, No. C1, pp. 492-498.

40) SYMONDS, G. and A.J. BOWEN(1984) : Interaction of nearshore bars with incoming wave groups, *J. Geophy. R.*, Vol.89, No.C2, pp. 1953-1959.

41) TAKAHASHI, T., M. HIROSE, K. SUGAHARA and N. HASHIMOTO (1981) : Wave statistics with 10-year data in the coastal wave observation network, *Technical Note of the Port and Harbour Research Institute*, Ministry of Transport, Japan, No. 401, 711p. (in Japanese).

42) TANAKA, N., H. OZASA and A. OGASAWARA, (1973) : Note of the investigations of shore line, Part 1, -The investigations on shoreline change on the basis of aerial photographs-, *Technical Note of the Port and Harbour Research Institute*, Ministry of Transport, Japan, No.163, 95p.(in Japanese).

43) TANAKA, N. and M. SAWAMOTO (1974a) : On shoreline change near harbours at sandy beaches, -Understanding of the present state on the basis of aerial photographs and an attempt of classification-, *Technical Note of the Port and Harbour Research Institute*, Ministry of Transport, Japan, No.180, 121 p.(in Japanese).

44) TANAKA, N., and H.OZASA(1974b) : Note of the investigations on changes of shorelines in Japan, Part 2, -The investigations on shoreline changes by using aerial photographs-, *Technical Note of the Port and Harbour Research Institute*, Ministry of Transport, Japan, No.192, 106p.(in Japanese).

45) TANAKA, N., H.OZASA, K. HACHISUKA and E. MIYOSHI(1977) : Note of the investigations on changes of shoreline in Japan, Part 3, -the investigations on shoreline changes by using aerial photographs-, *Technical Note of the Port and Harbour Research Institute*, Ministry of Transport, Japan, No.266, 159p. (in Japanese).

46) TUCKER, M.J.(1950) : Surf beats : Sea waves of 1 to 5 minute period, *Proc. Roy. Soc., London*, A.202, pp.565-573.

47) WRIGHT, L.D., B.G.THOM and J. CHAPPELL(1978) : Mophodynamic variability of high-energy beaches, *Proc. 16th Int. Conf. on Coastal Eng.*, pp.1180-1194.

Postscript

When this paper was in press, the author had a chance to see a manuscript of the paper[48] by Dr. Ishida and Dr. Yoshioka et al., Nagoya Institute of Technology, with their courtesy. They have been also studying on the multiple longshore bars in the beach near Hakui Beach. They took many samples of bed materials from the sea bed of the depth up to 15 meters along measurement lines normal to a shoreline. Their results of the analysis on the grain size distribution show that the medium diameter of sand is less than 0.2 millimeter around the crests, while it is about 3 to 4 millimeters at the troughs. This evinence is considered to support one of the conclusions of this paper that the suspended sand transport is predominant during the strom conditoin, because finer sediments are apt to be transported in suspension to the bar crests.

48) ISHIDA, A. and W. YOSHIOKA, et al(1984) : Field observafion on multiple longshore bars in Ishikawa Beach, *Proc. of 38th Annual Conf. on Civil Eng.*, *JSCE* (in Japanese).